Exploration of a Series of 5-Arylidene-2-thioxoimidazolidin-4-ones as Inhibitors of the Cytolytic Protein Perforin

Julie A. Spicer,*[†,‡] Gersande Lena,[†] Dani M. Lyons,[†] Kristiina M. Huttunen,[†,§] Christian K. Miller,[†] Patrick D. O'Connor,[†] Matthew Bull,[†,‡] Nuala Helsby,[†,‡] Stephen M. F. Jamieson,[†,‡] William A. Denny,[†,‡] Annette Ciccone,[‖] Kylie A. Browne,[‖] Jamie A. Lopez,[‖] Jesse Rudd-Schmidt,[‖] Ilia Voskoboinik,[‖] and Joseph A. Trapani[‖,⊥]

[†]Auckland Cancer Society Research Centre, Faculty of Medical and Health Sciences, The University of Auckland, Private Bag 92019, Auckland 1142, New Zealand

[‡]Maurice Wilkins Centre for Molecular Biodiscovery, A New Zealand Centre for Research Excellence, Auckland, New Zealand

[§]School of Pharmacy, Faculty of Health Sciences, University of Eastern Finland, P.O. Box 1627, FI-70211 Kuopio, Finland

[‖]Cancer Immunology Program, Peter MacCallum Cancer Centre, St. Andrew's Place, East Melbourne, Victoria 3002, Australia

[⊥]Sir Peter MacCallum Department of Oncology, The University of Melbourne, Parkville, Victoria 3052 Australia

S *Supporting Information*

ABSTRACT: A series of novel 5-arylidene-2-thioxoimidazolidin-4-ones were investigated as inhibitors of the lymphocyte-expressed pore-forming protein perforin. Structure–activity relationships were explored through variation of an isoindolinone or 3,4-dihydroisoquinolinone subunit on a fixed 2-thioxoimidazolidin-4-one/thiophene core. The ability of the resulting compounds to inhibit the lytic activity of both isolated perforin protein and perforin delivered in situ by natural killer cells was determined. A number of compounds showed excellent activity at concentrations that were nontoxic to the killer cells, and several were a significant improvement on previous classes of inhibitors, being substantially more potent and soluble. Representative examples showed rapid and reversible binding to immobilized mouse perforin at low concentrations (≤ 2.5 μM) by surface plasmon resonance and prevented formation of perforin pores in target cells despite effective target cell engagement, as determined by calcium influx studies. Mouse PK studies of two analogues showed $T_{1/2}$ values of 1.1–1.2 h (dose of 5 mg/kg iv) and MTDs of 60–80 mg/kg (ip).

in vitro HTS hit   *in vivo* candidates
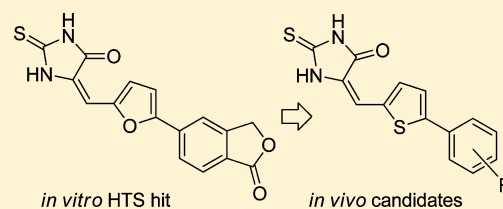
INTRODUCTION

The key effector cells of the immune system, cytotoxic T lymphocytes (CTL), and natural killer (NK) cells eliminate virus-infected and transformed cells principally through the granule exocytosis pathway.[1,2] CTLs and NK cells contain secretory vesicles (granules) that are used to store various cytotoxic proteins, including a group of proapoptotic serine proteases (granzymes)[3] and perforin, a pore-forming glyco-protein.[4–7] Stable conjugation with a target cell results in exocytic delivery of the granule contents into the immune synapse where perforin facilitates entry of the granzymes into the target cell, triggering various apoptotic death mechanisms.

The crystal structure of monomeric murine perforin has been determined to 2.75 Å resolution and reveals a bent and twisted four-stranded β-sheet MACPF domain flanked by two clusters of α-helices, an epidermal growth factor (EGF) domain, and a C-terminal C2 domain that mediates initial, calcium-dependent membrane-binding.[8] The mechanism of pore formation has also been elucidated; upon exposure of perforin to the neutral, calcium-rich extracellular environment of the immune synapse, deprotonation of key aspartate residues and subsequent coordination of calcium takes place. This process triggers

conformational changes that result in the assembly of highly ordered oligomers of 19–24 subunits that form a pore with an internal diameter of 130–200 Å. Site directed mutagenesis has established that direct ionic interactions between the opposing faces of adjacent perforin monomers (Arg213 and Glu343 in particular) serve to assist pore self-assembly and stabilization of the resulting pore.[8–10]

Perforin is encoded on a single-copy gene in both mice and humans,[3] and while many of the granule components possess at least some degree of redundancy, perforin is absolutely essential for protective immunosurveillance. Perforin knockout mice show a reduced ability to reject many tumor xenografts, and when backcrossed with nonobese diabetic mice, the incidence of spontaneous diabetes is reduced from 77% in a perforin +/+ control to 16% in perforin-deficient mice, with onset of disease markedly delayed. This is because perforin is critical to deliver an autoimmune "lethal hit" against the insulin-producing pancreatic β cells.[11] Perforin-deficient mice also demonstrate increased susceptibility and failure to clear many viruses and other

intracellular pathogens, and highly aggressive disseminated B cell lymphomas occur in the majority of animals over the age of 12 months.[12] In humans, complete loss of perforin function results in familial hemophagocytic lymphohistiocytosis (FHL) syndrome, a severe immunoregulatory disorder usually diagnosed in infancy and characterized by severe anemia and hepatosplenomegaly, fever, and thrombocytopenia.[13,14]

There is abundant evidence to implicate inappropriate perforin activity in a number of human pathologies, including cerebral malaria, insulin-dependent diabetes, juvenile idiopathic arthritis, and postviral myocarditis,[15−17] as well as therapy-induced conditions such as allograft rejection and graft-versus-host disease.[18−20] Immunosuppressive agents used to treat these diseases are generally associated with a wide range of side effects, many of which arise from the unintended impact of the drug treatment on nontherapeutic targets.[21,22] As perforin is expressed only by "killer lymphocytes", a selective inhibitor should result in fewer off-target effects, meaning a small molecule inhibitor of perforin is of great interest as a new class of highly specific immunosuppressive agents.[17]

In our initial work in this area, we explored two series of compounds (**1** and **2**, Figure 1) that showed appreciable
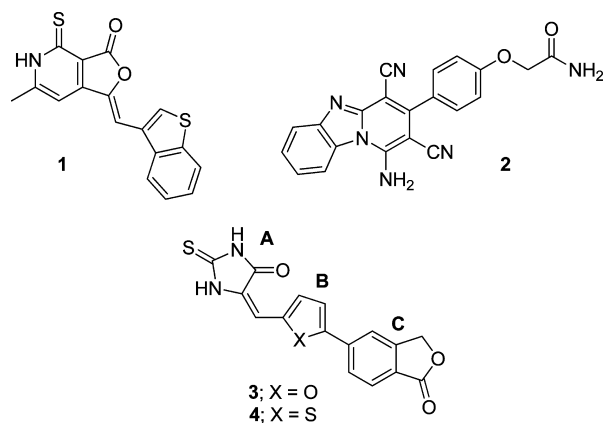
Figure 1. Published small-molecule inhibitors of perforin.

perforin-inhibitory activity but possessed limitations such as poor aqueous solubility or reduced activity in serum, precluding further development.[23,24] We have substantially overcome these issues in our current series of 5-arylidene-2-thioxoimidazolidin-4-one-based inhibitors (**3**, **4**)[25,26] and now seek to maximize inhibitory activity and optimize "druglike" properties. This class of rhodanine-related heterocycle has recently become the subject of considerable debate in the medicinal chemistry community because of several publications classifying such substructures as either "privileged scaffolds" with potentially valuable biomolecular binding properties[27−29] or "frequent/promiscuous hitters" and pan-assay interference compounds (PAINS) which should not be pursued further.[30−32] While it is clear that these chemotypes should be carefully monitored in development, recent literature contains many examples of selective inhibitors of various target proteins containing such substructures.[26,27,33,34] In addition, many of these moieties also occur in drugs that are clinically useful, providing templates with valuable structural features favoring protein binding which may be exploited in an advantageous way. Nevertheless, our current lead compound was subjected to and passed the PAINS filters[30] (Professor Jonathan Baell, personal correspondence)[35] possibly because of the presence of an extra nitrogen in the core five-membered ring.

Herein we will show that we have identified an exciting new class of inhibitors that unambiguously target perforin, offering up a novel mode of action and the potential to be further developed as immunosuppressive agents for the effective treatment of transplant rejection and selected autoimmune diseases.

■ RESULTS AND DISCUSSION

Lead compound **3** was selected from a small number of hits that showed reproducible perforin-inhibitory activity in a high throughput screen of approximately 100 000 compounds sourced from commercial libraries.[36] Compound **3** can be readily disconnected into three subunits, a 2-thioxoimidazolidin-4-one (A), a furan (B), and a benzofuranone (C), lending itself to a study design where one unit can be independently varied in the presence of two other fixed subunits. We have reported previously our study of the structure−activity relationships (SAR) resulting from variation of the A- and B-subunits,[26] and here we focus on the effect of introducing a wide range of C-subunits. Since thiophene **4** was one of the more potent compounds in our initial work, the current study explores the effect of replacing the benzofuranone C-subunit on a fixed 2-thioxoimidazolidin-4-one/thiophene scaffold. The requirement for substitution on the C-subunit aryl ring is explored, followed by a more detailed investigation focusing on compounds containing a bicyclic moiety.

Synthesis of Target Compounds. The compounds of Tables 1, 2, and 3 were prepared by heating a range of substituted aldehydes with 2-thioxoimidazolidin-4-one in acetic acid in the presence of β-alanine (Schemes 1−5). As a consequence, the majority of the chemistry that is described here involves the preparation of key aldehyde intermediates. For the compounds of Table 1, a small number of protected aldehydes (**6−8**) were prepared by Suzuki reaction of 2-(5-bromothiophen-2-yl)-1,3-dioxolane (**5**) with substituted phenylboronic acids, followed by deprotection (Scheme 1). The remaining aldehydes were commercially available with the exception of amides **34−42**, which were prepared from carboxylic acid **28** using standard amide coupling conditions. All the required aldehydes **9−42** were then converted to final compounds **43−75**.

Table 2 contains compounds where the benzofuranone of **3** has been replaced with a variety of substituted isoindolinones (**118−135**, **165**, **166**) and 3,4-dihydroisoquinolin-1(2H)-ones (**167−170**). The isoindolinone targets were prepared by bromination of methyl ester **76**, followed by ring closure onto a variety of amines to give intermediate iodides **77−81** (Scheme 2). These iodides were then employed in a palladium-catalyzed reaction using an AgNO$_3$/KF activator system, as originally described by Mori et al.[37] Coupling of the iodides with either 2-(thiophen-2-yl)-1,3-dioxolane or 2-(dimethoxymethyl)-thiophene at the vacant 5-position of the thiophene gave the desired protected aldehydes **82−86**. Compound **82** was further modified through NaH/RX alkylations of the isoindolinone NH to afford **87−92**. The NMe derivative **87** was alkylated a second time using LDA and methyl iodide to give methylation on the isoindolinone CH$_2$ (**93**) in 65% yield. Deprotections of **82−93** were carried out under acidic conditions to give the required aldehydes **94−106** which were then reacted with 2-thioxoimidazolidin-4-one to give final compounds **118−130** and **135**. Likewise **136** (Table 3) was obtained by reaction of aldehyde **82** with imidazolidine-2,4-dione. A small set of amino-substituted compounds (**131−134**) were also prepared from the C3 alcohol **101**. The aldehyde substituent of **101** was initially protected as the dimethyl acetal **107**. Then the alcohol converted to the

Table 1. Inhibitory Activities of C-Subunit Variants
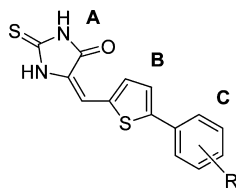
compd	R	inhibition of Jurkat cell lysis, IC$_{50}$ (μM)[a]
4	see Figure 1	0.78
43	H	>20
44	2-Cl	>20
45	3-Cl	7.19
46	4-Cl	5.22
47	3-F	10.77
48	4-F	6.69
49	3,4-di-F	4.59
50	3-CF$_3$	5.66
51	4-CF$_3$	4.66
52	3-CN	9.68
53	4-OH	7.72
54	3-CF$_3$, 4-Cl	3.09
55	4-Br	1.69
56	4-SMe	1.15
57	4-Ac	1.67
58	4-CH$_2$OAc	3.04
59	4-COOMe	1.62
60	3-CONH$_2$	0.79
61	4-CONH$_2$	1.56
62	3-Me, 4-COOMe	3.03
63	4-SO$_2$Me	13.80
64	4-NHSO$_2$Me	7.70
65	3-pyridyl	12.89
66	4-pyridyl	10.06
67	4-CONHMe	4.53
68	4-CONMe$_2$	6.93
69	4-COMorpholine	>20
70	4-CONH(CH$_2$)$_2$morpholine	>20
71	4-CONH(CH$_2$)$_3$morpholine	8.13
72	4-CONH(CH$_2$)$_2$OH	3.64
73	4-CONH(CH$_2$)$_3$OH	4.35
74	4-CONHCH$_2$CH(CH$_3$)OH	6.50
75	4-CONHCH$_2$CH(OH)CH$_2$OH	2.44

[a]Testing was carried out over a range of concentrations, with the IC$_{50}$ being equal to the concentration at which 50% inhibition of the lysis of Jurkat cells by purified recombinant perforin was observed, as measured by ^{51}Cr release. Values are the average of at least three independent IC$_{50}$ determinations.

mesylate **108** using mesyl chloride and TEA in THF. The mesylate was exchanged for iodide by heating with a large excess of NaI in acetone. Then the iodide of **109** was displaced with various amines to give intermediates **110−113**. Deprotection as described above gave the key aldehydes **114−117** which were reacted with 2-thioxoimidazolidin-4-one to give final compounds **131−134**.

Scheme 3 describes the preparation of "reverse" and five- and six-membered lactams **165−170** (Table 2). The five-membered lactam boronates **147** and **148** were prepared from the corresponding bromides **137** and **138** by Pd-catalyzed reaction with bis(pinacolato)diboron. The four six-membered lactam boronates **149−152** were prepared in the same manner from the

bromides **143−146** which were in turn synthesized from the carbamates **139−142** according to literature procedures.[38,39] The boronates were then each employed in a Suzuki reaction with bromide **5** to give compounds **153−158** which were deprotected and reacted with 2-thioxoimidazolidin-4-one to afford final compounds **165−170**. For comparison with the isoindolinones, a single indole-based compound, 3-acetylindole **178**, was also prepared (Scheme 4). 5-Bromoindole **171** was protected and acetylated according to literature procedures,[40,41] followed by displacement of the benzenesulfonyl protecting group to give the corresponding N-methylindole **174**. Subsequent Suzuki coupling, deprotection, and reaction with 2-thioxoimidazolidin-4-one gave target compound **178**.

For the compounds of Table 3, protected bromothiophene- (**179**), bromobenzene- (**180**, **181**), bromopyridine- (**182**), bromoindole- (**183**, **184**), or bromoquinolone- (**185**) carboxaldehydes were reacted with either commercially available 5-(4,4,5,5-tetramethyl-1,3,2-dioxaborolan-2-yl)isoindolin-1-one or boronate **149** as described above, deprotected to aldehydes **195−203**, and converted to final products **204−212** (Scheme 5).

In Vitro Activities of the 5-Arylidene-2-thioxoimidazolidin-4-ones. In the first instance, the isobenzofuran-1(3H)-one C-subunit was replaced with a large range of substituted-benzene derivatives (Table 1). Substitution on this ring is clearly required, with phenyl (**43**) possessing no detectable activity. Each position was then surveyed with a range of substituents, and while methyl and methoxy proved to be inactive (see Supporting Information), a variety of electron-withdrawing substituents (halogen, CF$_3$, cyano, hydroxyl, carboxyl) did produce activity. The results for a series of chloro (**44−46**), fluoro (**47**, **48**), and CF$_3$ (**50**, **51**) compounds show a clear preference for substitution at the 4-position. Carboxy-based examples (**59−61**) were among the most potent, although in this instance the 3-carboxamide (**60**, IC$_{50}$ = 0.79 μM) was slightly better than its 4-isomer (**61**, IC$_{50}$ = 1.56 μM). Methylation of the carboxamide NH of **61** resulted in a reduction of activity (**67**, **68**), while amide-linked weakly basic side chains (**69−71**) were generally poor. The corresponding amide-linked hydroxylated side chains (**72−75**), however, exhibited significant activity (IC$_{50}$ = 2.44−4.35 μM) but were still not as potent as the primary amide **61**. Other compounds with good activity were the 4-Br (**55**, 1.69 μM), 4-SMe (**56**, 1.15 μM), and 4-acetyl (**57**, 1.67 μM). The "acyclic" analogue of **4**, compound **62**, showed a 4-fold reduction in activity over its cyclic counterpart (IC$_{50}$ = 3.03 μM compared to 0.78 μM).

Although the above study (Table 1) produced some potent compounds, none were an improvement on lead compound **4**. An alternative approach where the entire isobenzofuran-1(3H)-one unit was replaced with an isoindolin-1-one was therefore implemented (Table 2), resulting in a series of compounds considered less susceptible to hydrolysis (amide versus ester) and where the nitrogen atom provides an additional position at which a side chain can be appended.

Isoindolin-1-one **118** showed a reduction of activity over lactone **4** (from IC$_{50}$ = 0.78 μM to IC$_{50}$ = 2.55 μM). Activity was restored through substitution on the nitrogen atom, with both methyl-substituted (**119**, IC$_{50}$ = 0.51 μM) and ethyl-substituted (**120**, IC$_{50}$ = 0.60 μM) compounds more potent than the lead compound **4**. A more bulky substituent such as isopropyl (**123**, IC$_{50}$ = 4.42 μM) was less acceptable, but the acetate **128** and carbamate **129** both showed excellent activity (IC$_{50}$ = 0.93 and 0.55 μM, respectively). In this series it also appears possible to introduce various side chains off the isoindolinone and maintain activity, with the two alcohols **125** and **126** among the most

Table 2. Inhibitory Activities of Lactam C-Subunits
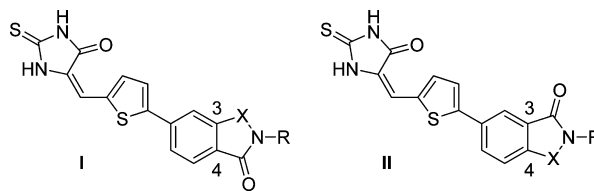
compd	structure	X	R	inhibition of Jurkat cell lysis, IC_{50} (μM)[a]
118[b]	I	CH_2	H	2.55
119	I	CH_2	Me	0.51
120	I	CH_2	Et	0.60
121	I	CH_2	n-Pr	1.52
122	I	CH_2	n-Bu	1.18
123	I	CH_2	i-Pr	4.42
124	I	CH_2	CH_2CH_2OAc	1.17
125	I	CH_2	CH_2CH_2OH	0.78
126	I	CH_2	$CH_2CH_2CH_2OH$	0.53
127	I	CH_2	$CH_2CH(OH)CH_2OH$	1.26
128	I	CH_2	Ac	0.93
129	I	CH_2	C(O)OEt	0.55
130	I	CH_2	CH_2CH_2morph	variable
131	I	CH_2	$CH_2CH_2CH_2NMe_2$	>20
132	I	CH_2	$CH_2CH_2CH_2$piperidine	11.78
133	I	CH_2	$CH_2CH_2CH_2NMe$piperazine	>20
134	I	CH_2	$CH_2CH_2CH_2$pyrrolidine	8.93
135	I	$CH(CH_3)$	Me	3.21
165[c]	II	CH_2	H	1.38
166	II	CH_2	Me	1.89
167	I	$(CH_2)_2$	H	1.14
168	II	$(CH_2)_2$	H	0.64
169	I	$(CH_2)_2$	Me	2.33
170	II	$(CH_2)_2$	Me	4.76
178[d]				5.30

[a]Testing was carried out over a range of concentrations, with the IC_{50} being equal to the concentration at which 50% inhibition of the lysis of Jurkat cells by purified recombinant perforin was observed, as measured by ^{51}Cr release. Values are the average of at least three independent IC_{50} determinations. [b]Preparation of compounds **118−135** described in Scheme 2. [c]Preparation of compounds **165−170** described in Scheme 3. [d]Compound **178** contains a 3-acetylindole C-subunit, and its synthesis is described in Scheme 4.
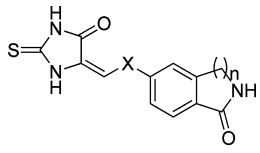
potent compounds of the class (IC_{50} = 0.78 and 0.53 μM). Diol **127** and O-acetate **124** also demonstrated good activity, but when a basic amino substituent was introduced in an attempt to improve solubility, activity was virtually abolished with only morpholine (**130**, not reproducible), piperidine **132**, and pyrrolidine **134** (IC_{50} = 11.78 and 8.93 μM) showing any evidence of activity. Introduction of a methyl substituent on the lactam ring (**135**) resulted in poorer activity than the corresponding unsubstituted analogue (**135** IC_{50} = 3.21 μM vs **119** IC_{50} = 0.51 μM).

Since the 3-carboxamide **60** was 2-fold more potent than 4-carboxamide **61** in the substituted benzene series (Table 1), the effect of reversing the orientation of the lactam ring was investigated (**165**). The same result was observed; the IC_{50} for the compound with the lactam amide in the 3-position **165** (relative to the thiophene) was around 2-fold better than the corresponding lactam amide in the 4-position (**118**) (IC_{50} = 1.38 μM compared to 2.55 μM). Expansion from a five-membered lactam ring (**118**) to a six-membered lactam ring (**167**) also resulted in a significant increase in activity (from IC_{50} = 2.55 to IC_{50} = 1.14 μM) and improved a further 2-fold (to 0.64 μM) through introduction of the "reverse" 3-lactam amide (**168**). N-Methylation of **165**, **167**, and **168** to give **166**, **169**, and **170**, respectively, did not result in the same increase in activity seen

when **118** was alkylated to give the analogous N-methyl compound **119**.

Compounds **136** and **204−212** (Table 3) combine those B-subunits which were previously identified as having excellent activity in the isobenzofuranone-based series,[26] with selected isoindolinones and 3,4-dihydroisoquinolin-1(2H)-ones from the current series. Compound **136** contains a imidazolidine-2,4-dione A-subunit and is the only example to show an improvement, being 3-fold better than the analogous isobenzofuranone reported in our initial paper (IC_{50} = 0.40 μM compared to 1.19 μM). All other compounds (**204−212**) contain a 2-thioxoimidazolidin-4-one A-subunit and are 1.5- to 4-fold poorer than the corresponding isobenzofuranones (see Figure 1 in Supporting Information).

Those compounds that showed good inhibition of the purified protein were then also evaluated for their ability to inhibit perforin produced by an intact NK cell line (KHYG-1; see Experimental Section for details); this assay is a better model for in vivo studies, as the perforin is delivered by a functional NK cell. To confirm that inhibition of NK cell function was due to blocking the action of perforin and not nonspecific toxicity against the effector cell, viability was also measured 24 h after the NK cells were exposed to the compounds (4 h, 37 °C), then washed and replated in culture. Elimination of any nonspecific

Table 3. Inhibitory Activities of Optimized A-, B-, and C-Subunits

compd	X^a	n	inhibition of Jurkat cell lysis, IC$_{50}$ (μM)^b
136	2,5-thiophene^c	1	0.40
204	2,4-thiophene	1	3.00
205	1,4-benzene	1	5.55
206	1,3-benzene	1	3.44
207	3,6-pyridine	1	0.63
208	2,6-(1H-indole)	1	1.58
209	2,5-(1H-indole)	1	2.50
210	2,6-(1H-indole)	2	1.66
211	2,5-(1H-indole)	2	1.45
212	2,6-quinoline	2	2.55

^{a}Structure of the B-subunit. ^{b}Testing was carried out over a range of concentrations, with the IC$_{50}$ being equal to the concentration at which 50% inhibition of the lysis of Jurkat cells by purified recombinant perforin was observed, as measured by ^{51}Cr release. Values are the average of at least three independent IC$_{50}$ determinations. ^{c}The 2-thioxoimidazolidin-4-one A-subunit is replaced with a imidazolidine-2,4-dione.

toxicity is important because CTLs and NK cells play a key role in the overall immunological response, meaning that any potential perforin-targeted treatment must allow rapid recovery of these cytotoxic effector cells. For the purposes of this study, compounds were classified as toxic if NK cell viability fell below 70% at 24 h.

The data contained in Table 4 were used to identify compounds suitable for advancement into in vivo pharmacokinetic studies, as a prelude to in vivo efficacy testing. In the absence of serum, the majority of compounds possessed similar or improved inhibitory activity compared to previous lead **4**, notably **118**, **135**, and **167**, which all showed excellent activity in this more demanding system (56%, 90%, 83% compared to 53%). As reported with previous series,[26] a number of compounds were adversely affected in the presence of serum, precluding their further consideration (**125**, **126**, **129**, **168**, **207**). The solubility of all compounds was substantially improved by their conversion to sodium salts, resulting in an enhanced drug profile, although some examples (**118**, **119**, **129**, **136**, **168**) still proved too insoluble in this form for administration in vivo. Compounds **119** and **167** also showed some evidence of toxicity toward the NK cells (28% and 38% survival at 20 μM, respectively). The compound with the best overall profile for an in vivo candidate was **135**, combining superior activity in the

presence and absence of serum (90% and 67%, respectively) with good viability (74%) and aqueous solubility (1408 μg/mL). In addition, when **167** was tested at a lower concentration of 5 μM, the resultant lack of NK toxicity suggested a possible therapeutic window, meaning this compound was also selected as an in vivo candidate.

In Vivo Pharmacokinetics of Selected Compounds. Compounds **135** and **167** were evaluated for plasma pharmacokinetics in male CD-1 mice. Blood samples were collected at multiple time-points after dosing at 5 mg/kg in a solution of 20% hydroxypropyl-β-cyclodextrin by intravenous injection. Both compounds were determined to have acceptable drug exposures (AUC = 1151 and 955 h·ng/mL, respectively), despite high clearance and volume of distribution values (Table 5). On this basis, **135** and **167** were progressed to maximum tolerated dose (MTD) studies by single or multiple doses (intraperitoneally) to establish an appropriate level for efficacy studies. Both compounds were found to be well tolerated after a single dose of 80 and 60 mg/kg, respectively, while when administered twice daily over 3 days, 60 and 40 mg/kg were found to be suitable for multiple dosing.

Binding Affinity of Inhibitors to Perforin Protein. While several series of potent inhibitors have now been identified,[23−26] little is known about the mechanism by which the cytolytic activity of perforin action is blocked. In order to find out more about the nature and degree of inhibitor binding, recombinant purified mouse perforin was immobilized on a surface plasmon resonance (SPR) S-series CM5 sensor chip using standard amide coupling methodology. Then solutions of in vivo candidates **135** and **167** in buffer were passed over the covalently bound protein, and relative binding affinities were determined using a Biacore T200 SPR machine.

Inhibitors **135** and **167** were found to bind reversibly to the immobilized perforin, and during injection a steady-state response was achieved within seconds (Figures 2 and 3 in Supporting Information). At the end of the injection the compounds dissociated rapidly with an almost immediate return to baseline resonance response. Any nonspecific binding to the sensor chip surface was accounted for through the response in the reference flow cell. Because of the relative insolubility of the compounds in the running buffer, low analyte concentrations were required (≤2.5 μM) and the relative resonance responses at steady state were typically below 10 response units (RU). However, although the absolute response values were low, it is clear that **135** and **167** can bind to perforin even at low concentrations. These data demonstrate for the first time that these inhibitors possess the ability to bind reversibly to perforin monomers. Prior to this experiment it was also not known whether immobilization of perforin monomers to the sensor chip surface via (random) amide couplings could render potential

Scheme 1^a
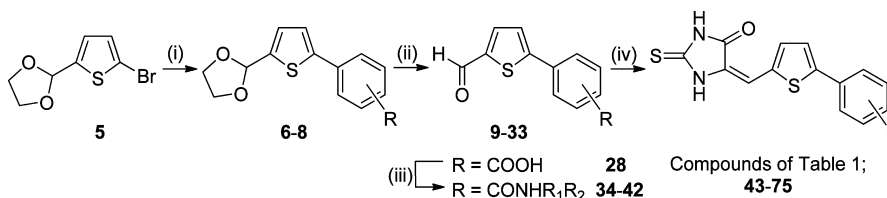
^{a}Reagents and conditions: (i) R-phenylboronic acid, 2 M Na$_2$CO$_3$, toluene/EtOH, PdCl$_2$(dppf), reflux, 2 h; (ii) 1 M HCl, acetone, rt; (iii) (a) PFP−TFA, pyridine, THF, rt, (b) R$_1$R$_2$NH, THF, rt; (iv) 2-thioxoimidazolidin-4-one, β-alanine, AcOH, reflux, 15 h.

Scheme 2[a]
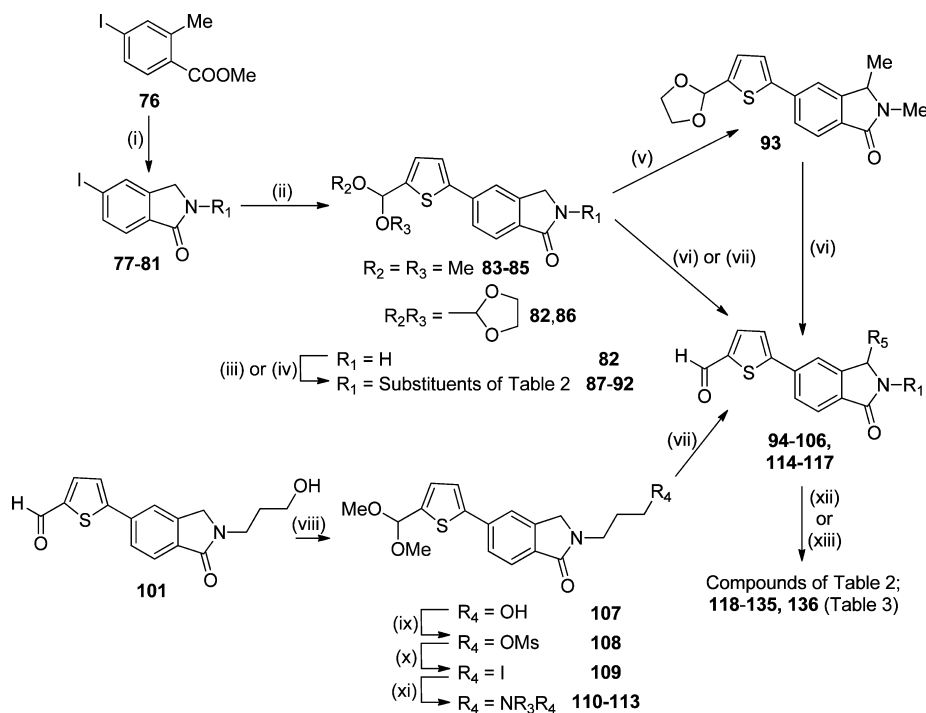
[a]Reagents and conditions: (i) (a) NBS, AIBN, benzene, reflux, 6 h, (b) R_1NH_2, THF, rt; (ii) 2-(thiophen-2-yl)-1,3-dioxolane or 2-(dimethoxymethyl)thiophene, PdCl$_2$(PPh$_3$)$_2$, KF, AgNO$_3$, DMSO, 100 °C, 2 h; (iii) (a) NaH, DMF, 0 °C to rt, (b) R_1X, DMF, rt, 1 h; (iv) Ac$_2$O, reflux, 2 h; (v) (a) LDA, THF, −78 °C, 0.25 h, (b) MeI, THF, −78 °C-rt; (vi) 1 M HCl, acetone, rt; (vii) p-TsOH, acetone/water, 50 °C, 5 h; (viii) (MeO)$_3$CH, p-TsOH, 4 Å molecular sieves, MeOH, reflux, 15 h; (ix) MsCl, TEA, THF, rt; (x) NaI, acetone, 70 °C, 1 h; (xi) R$_2$R$_3$NH, DMA, rt.; (xii) 2-thioxoimidazolidin-4-one, β-alanine, AcOH, reflux, 15 h; (xiii) hydantoin, β-alanine, AcOH, reflux, 15 h (**136**).

binding sites for inhibitors inaccessible. Combined, these findings show that SPR biosensor analysis can be a useful technique to determine perforin protein–drug binding interactions.

Investigation of the Mechanism of Perforin Inhibition. In order to investigate whether **167** inhibited perforin directly in the context of the physiological immune synapse, we also used real-time microscopy to analyze the functional interaction between primary human natural killer cells and their cognate model targets, HeLa cells. When the killer cell engages with its target cell, a cascade of downstream signaling events leads to the influx of extracellular Ca^{2+} (as detected by the calcium ionophore Fluo-4). As shown recently,[42] Ca^{2+} influx directly precedes degranulation and the release of perforin into the synaptic cleft. Perforin then forms pores in the target cell membrane, which can be detected as an influx of extracellular propidium iodide (PI), a dye that gains fluorescence upon binding to the cytosolic RNA.[42] Calcium influx into the killer cell and PI uptake by the target cell thus serve as indicators of a functional immune synapse. In the DMSO-treated control cells, every natural killer cell that engaged with its target cell ($n = 50$ cells) delivered functional perforin to the target (Figure 2). By contrast, in the presence of 20 μM **167**, only 60% of killer cells delivered functional perforin to the target. Formation of the perforin pore was blocked in the remaining 40% of synapses, despite effective target cell engagement (Figure 2). These data demonstrate that **167** directly inhibits perforin-induced lysis through reduction of cell membrane binding and/or prevention of transmembrane pore formation, thus preventing target cell death.

■ CONCLUSIONS

The current study has resulted in further optimization of a novel new series of small-molecule inhibitors of the pore-forming protein perforin. By building on our previous studies,[26] we have designed compounds that possess enhanced druglike properties compared to earlier structures. We also report new mechanistic evidence that reveals a specificity for the granule exocytosis pathway, of which perforin is an integral component.

Structure–activity relationships for variation of the C-subunit on a 2-thioxoimidazolidin-4-one/thiophene scaffold showed a need for substitution, especially at the 4-position, for simple substituted-benzene derivatives (Table 1). In this series the 3- and 4-carboxamides **60** and **61** proved to be the most potent, although this was limited to primary amides, as the introduction of N-substitution and extended hydroxyalkyl or aminoalkyl side chains (**67−75**) resulted in a loss of activity. The "acyclic" analogue of the lead compound (**62**) also showed an almost 4-fold reduction in activity, suggesting retention of a bicyclic C-subunit to be the best approach. The isobenzofuranone of **4** was therefore replaced with a variety of isomeric isoindolinones and 3,4-dihydroisoquinolin-1(2H)-ones. N-Substitution on the isoindolinone nitrogen was beneficial, with methyl (**119**), ethyl (**120**), hydroxyethyl (**125**), and hydroxypropyl (**126**) substituents all demonstrating excellent activity (IC$_{50}$ = 0.51, 0.60, 0.78, 0.53 μM, respectively). Comparable substitution on the 3,4-dihydroisoquinolin-1(2H)-one nitrogen did not improve activity (comparing **167**/**169** and **168**/**170** pairings), although these compounds (**167**, **168**) still showed potent inhibitory activity in their own right. Lastly, a series of hybrid compounds were prepared (Table 3), combining B-subunits that were previously identified as conferring good activity[26] with the above optimized

Scheme 3[a]
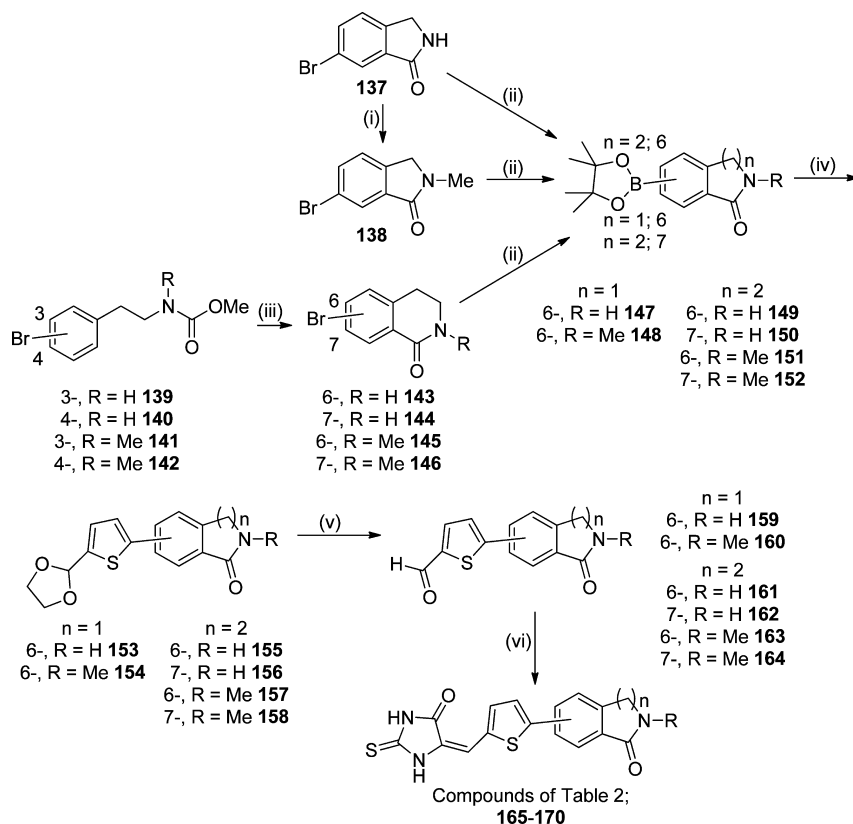
[a]Reagents and conditions: (i) (a) NaH, DMF, 0 °C to rt, (b) MeI, DMF, rt, 1 h; (ii) bis(pinacolato)diboron, KOAc, Pd(dppf)Cl$_2$, DMSO, 90 °C, 5 h; (iii) P$_2$O$_5$, POCl$_3$, reflux, 2 h; (iv) 5, 2 M Na$_2$CO$_3$, toluene/EtOH, PdCl$_2$(dppf), reflux, 2 h; (v) 1 M HCl, acetone, rt; (vi) 2-thioxoimidazolidin-4-one, β-alanine, AcOH, reflux, 15 h.

Scheme 4[a]
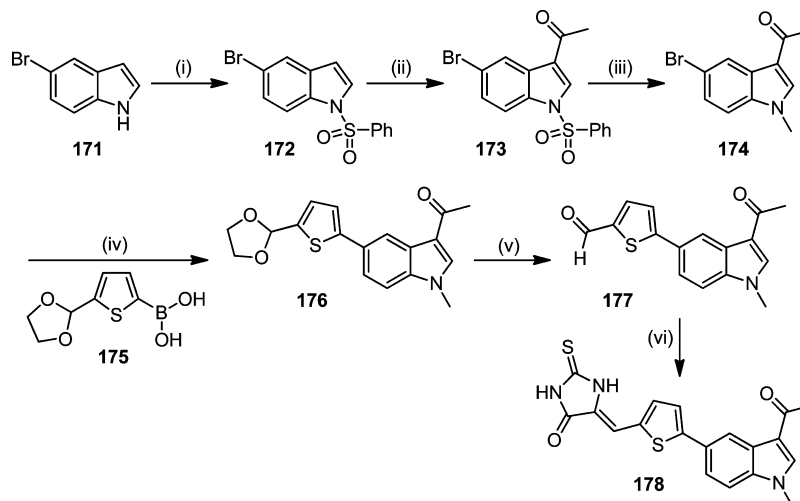
[a]Reagents and conditions: (i) PhSO$_2$Cl, NaOH, Bu$_4$N$^+$HSO$_4^-$, CH$_2$Cl$_2$, rt; (ii) Ac$_2$O, AlCl$_3$, CH$_2$Cl$_2$, rt; (iii) MeOH, Bu$_4$N$^+$Br$^-$, CsCO$_3$, toluene, 65 °C, 1 h; (iv) 2 M KHCO$_3$/DMF (3:1), Pd(dppf)Cl$_2$, 70 °C, 1 h; (v) acetone/2 M HCl (3:1), rt; (vi) 2-thioxoimidazolidin-4-one, β-alanine, AcOH, reflux, 15 h.

C-subunits. In this instance, the isoindolinones were all poorer than the corresponding isobenzofuranones (Figure 1 of Supporting Information).

A smaller subset of active compounds were then screened for their ability to inhibit perforin-dependent lysis induced by whole NK cells, resulting in the selection of 135 and 167 as suitable candidates for in vivo studies. Problems observed previously, such as poor aqueous solubility, inactivity in serum, and toxicity have been substantially overcome in the present series.

The mechanism of perforin inhibition by these compounds has also been investigated further, and for the first time, compounds with in vitro inhibitory activity have been shown to

Scheme 5[a]
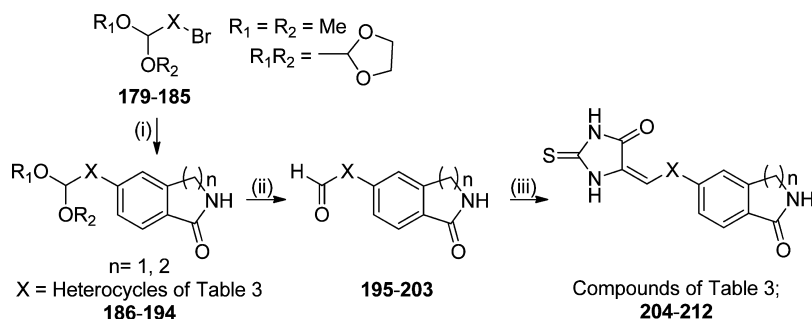
[a]Reagents and conditions: (i) 5-(4,4,5,5-tetramethyl-1,3,2-dioxaborolan-2-yl)isosindolin-1-one or **149**, 2 M Na$_2$CO$_3$, toluene/EtOH, PdCl$_2$(dppf), reflux, 2 h; (ii) p-TsOH, acetone/water, 50 °C, 5 h; (iii) 2-thioxoimidazolidin-4-one, β-alanine, AcOH, reflux, 15 h.

Table 4. Additional Testing on Selected Compounds

compd	Jurkat IC$_{50}$ (μM)	KHYG-1 inhibition (% at 20 μM) no serum[a]	KHYG-1 inhibition (% at 20 μM) 10% serum[b]	KHYG-1 viability (%)[c]	solubility (μg/mL) [sodium salt]
4	0.78	53 ± 2.6	38.9 ± 3.5	88 ± 3.0	23.0 [43.0]
118	2.55	56 ± 7.2	55 ± 6.5	95 ± 3.5	0.54 [140]
119	0.51	42 ± 5.5	37 ± 2.4	28 ± 1.5	0.13 [151]
125	0.78	43 ± 5.8	24 ± 3.4	81 ± 0.5	43.0 [3429]
126	0.53	48 ± 7.9	17 ± 3.0	90 ± 3.0	1.78 [10187]
129	0.55	46 ± 5.9	35 ± 9.5	93 ± 4.1	0.18 [397]
135	3.21	90 ± 4.0	67 ± 6.1	74 ± 8.3	1.32 [1408]
136	0.40	49 ± 9.8	50 ± 7.1	93 ± 3.0	11.6 [136]
167	1.17	83 ± 4.6	81 ± 5.3	38 ± 7.8	0.53 [1573]
167[d]		51 ± 4.2	34 ± 6.4	82 ± 3.6	
168	0.64	51 ± 4.0	23 ± 7.1	87 ± 4.1	0.13 [37.2]
207	0.63	43 ± 5.4	13 ± 3.8	92 ± 2.6	0.59 [−][e]

[a]Inhibition by compounds (20 μM) of the perforin-induced lysis of K562 target cells when co-incubated with KHYG-1 human NK cells (see Experimental Section). Percent inhibition calculated compared to untreated control. [b]As for footnote a, but in the presence of 10% mouse serum. [c]Viability of KHYG-1 NK cells after 24 h by Trypan blue exclusion assay (see Experimental Section). All results are the average of at least three separate determinations ± SEM. [d]Compound 167 was also tested at 5 μM to test for activity under less toxic conditions. [e]Insufficient material to prepare sodium salt.

reversibly bind perforin by SPR detection. Real-time imaging of natural killer−target cell interaction demonstrates that the compounds block perforin within the immunological synapse and prevent target cell death but have no effect on the stability of immune synapse formation between the two cells. These inhibitors almost certainly target perforin after its release into the immune synapse, consistent with the fact that the original screen through which the inhibitors were identified featured the use of purified perforin protein rather than perforin delivered by an intact killer cell.

Together, the data we have amassed demonstrate that this series of compounds are selective inhibitors of perforin and not nonspecific promiscuous binders. We have previously shown that these compounds do not inhibit the mechanistically related pore-forming protein pneumolysin and that we observe a wide range of activities (0.36 to >20 μM) against both isolated perforin and perforin produced by whole NK cells.[26] Furthermore, the membrane-piercing terminal components of the mammalian membrane attack complex of complement (MAC), which share significant structural similarity with perforin and alternative, receptor-mediated proapoptoic pathways used by cytotoxic lymphocytes, are not inhibited (data not shown). These observations are recapitulated in the current report by the clear SAR demonstrated by the C-subunit (IC$_{50}$ of 0.51 to >20 μM), irrespective of the presence of a 5-arylidene-2-thioxoimidazolidin-4-one as the A-subunit. A range of activities was also observed against perforin released by intact NK cells, a far more rigorous model that requires the compound to block perforin released into the immunological synapse that transiently forms between the killer cell and its target.[43] Our live cell imaging analyses clearly show for the first time that perforin operating within a functional immune synapse, an intricate microenvironment comprising many proteins taking part in various complex signaling pathways, can be selectively targeted to inhibit perforin-dependent apoptosis of the target cell.

In summary, we have taken significant steps toward elucidating the role of perforin in the granule exocytosis pathway, using small-molecule inhibitors to investigate binding affinity and probe the mechanism of membrane interaction and subsequent pore formation. We have found compounds 135 and 167 to be both potent and soluble inhibitors of perforin in vitro. These compounds also possess appropriate in vivo pharmacokinetic characteristics and toxicity profiles for their selection as in vivo efficacy candidates in our pursuit of a novel class of perforin

Table 5. In Vivo Pharmacokinetics of Compounds 135 and 167[a]

compd	$T_{1/2}$ (h)	C_{max} (ng/mL)	AUC$_{0-\infty}$ (h·ng/mL)	V (mL/kg)	Cl (mL h^{-1} kg^{-1})
135	1.15	4488	1151	1478	4346
167	1.30	4513	955	2750	5237

[a]Pharmacokinetic parameters derived from the plasma concentration−time profiles for each compound following a 5 mg/kg iv dose. The results were processed using a bolus iv dose and two-compartment model with Phoenix WinNonlin 6.2 (Pharsight Corporation, St. Louis, MO). The derived parameters are maximum plasma concentration (C_{max}), the area under the curve (AUC), plasma half-life ($T_{1/2}$), volume of distribution (V), and clearance (Cl).
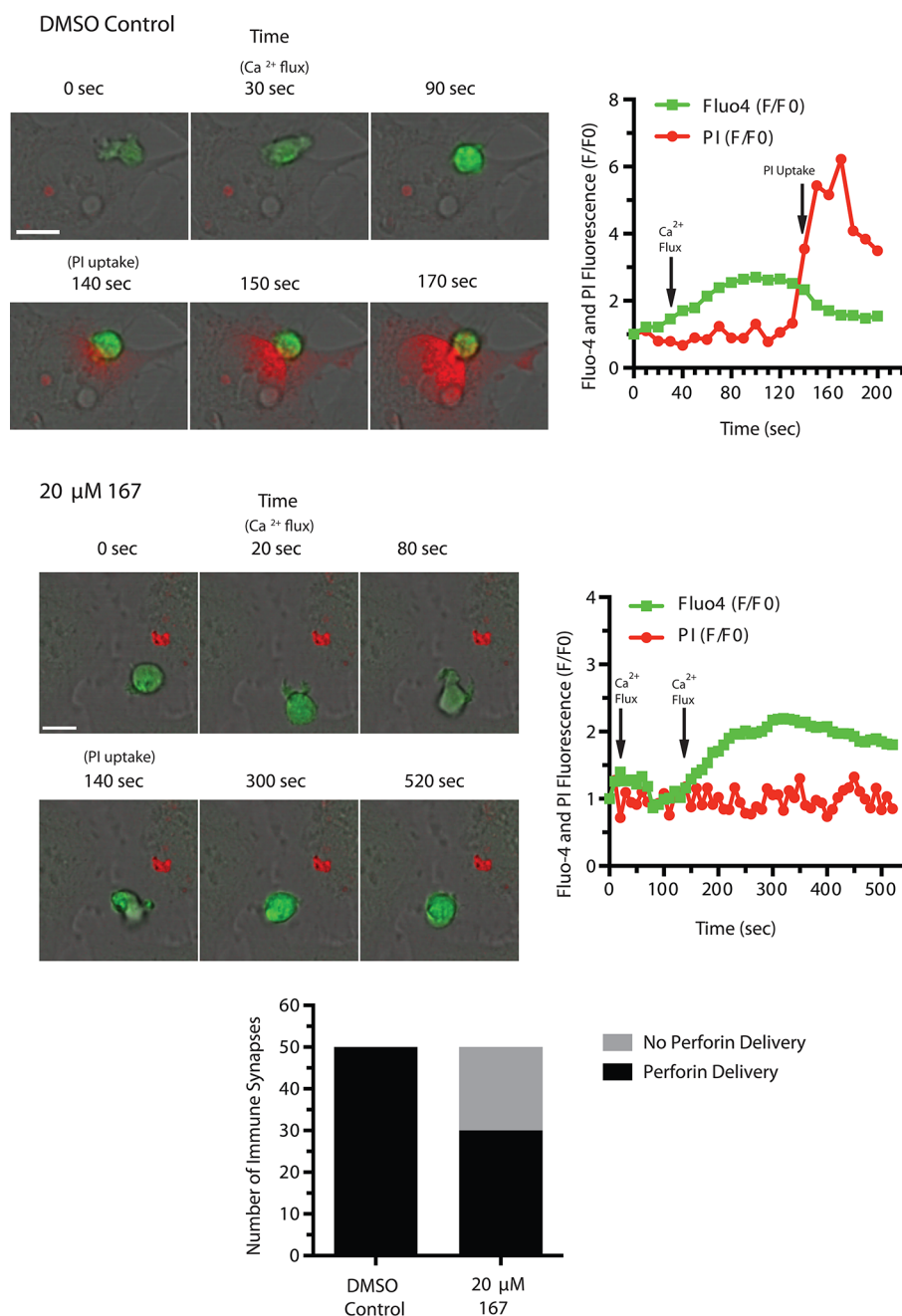
Figure 2. Effect of **167** in the context of the physiological immune synapse.

inhibitors suitable for the effective treatment of autoimmune-based diseases and transplant rejection.

◼ EXPERIMENTAL SECTION

Medicinal Chemistry. Analyses were performed by the Microchemical Laboratory, University of Otago, Dunedin, New Zealand. Melting points were determined using an Electrothermal model 9200 and are as read. NMR spectra were measured on a Bruker Avance 400 spectrometer and referenced to Me$_4$Si. Mass spectra were recorded either on a Varian VG 7070 spectrometer at nominal 5000 resolution or a Finnigan MAT 900Q spectrometer. All final compound purities were determined to be >95% by HPLC.

Representative general procedures are given below. Full experimental information for all remaining final compounds and intermediates is given in Supporting Information.

General Procedure A: (4-(5-(1,3-Dioxolan-2-yl)thiophen-2-yl)phenyl)methanol (6) (Scheme 1, R = CH₂OH). 5-Bromo-2-thiophenecarboxaldehyde was protected as the cyclic acetal **5** according to a literature procedure.[44] The acetal **5** (278 mg, 1.18 mmol) was then dissolved in toluene (12 mL), to which was added a suspension of 4-(hydroxymethyl)benzeneboronic acid (150 mg, 0.99 mmol) in EtOH (4 mL). A solution of 2 M Na$_2$CO$_3$ (3 mL) and Pd(dppf)Cl$_2$ (40 mg, 0.05 mmol) was added, and the entire mixture was heated at reflux under nitrogen for 2 h. When the mixture was cooled, all solvents were removed under reduced pressure and the resulting residue was partitioned between water (50 mL) and CH$_2$Cl$_2$ (50 mL). Two further CH$_2$Cl$_2$ (50 mL) extractions were performed. Then the combined organic fractions were dried (Na$_2$SO$_4$), filtered, and the solvent was removed under reduced pressure to afford a residue which was purified by flash column chromatography on silica gel (20% EtOAc/hexanes as eluant) to give **6** as a pale yellow solid (171 mg, 66%). ^{1}H NMR [400 MHz, (CD$_3$)$_2$SO] δ 7.60 (d, J = 8.3 Hz, 2 H), 7.36 (d, J = 3.6 Hz, 1 H), 7.35 (d, J = 8.4 Hz, 2 H), 7.20 (d, J = 3.8 Hz, 1 H), 6.04 (s, 1 H), 5.19 (t, J = 5.6 Hz, 1 H), 4.51 (d, J = 5.5 Hz, 2 H), 4.10−4.07 (m, 2 H), 3.93−4.00

(m, 2 H). LRMS (APCI$^+$) calcd for C$_{14}$H$_{15}$O$_3$S 263 (MH$^+$), found 263. This material contained ∼5% of deprotected aldehyde which was carried into the next step.

General Procedure B: 5-(4-(Hydroxymethyl)phenyl)-thiophene-2-carbaldehyde (24) (Scheme 1, R = CH$_2$OH). Compound **6** (171 mg, 0.65 mmol) was dissolved in acetone (10 mL), to which was added 1 M HCl (2 mL). This mixture was stirred at room temperature for 6 h, then concentrated under reduced pressure to afford a pale yellow suspension which was extracted into CH$_2$Cl$_2$ (2 × 50 mL). The combined organic fractions were evaporated down to give **24** as a yellow solid (142 mg, 100%). ^{1}H NMR [400 MHz, (CD$_3$)$_2$SO] δ 9.90 (s, 1 H), 8.03 (d, J = 3.9 Hz, 1 H), 7.76 (d, J = 8.3 Hz, 2 H), 7.72 (d, J = 4.0 Hz, 1 H), 7.42 (d, J = 8.4 Hz, 2 H), 5.26 (t, J = 5.7 Hz, 1 H), 4.54 (d, J = 5.6 Hz, 2 H). LRMS (APCI$^+$) calcd for C$_{12}$H$_{11}$O$_2$S 219 (MH$^+$), found 219.

General Procedure C: (E,Z)-4-(5-((5-Oxo-2-thioxoimidazoli-din-4-ylidene)methyl)thiophen-2-yl)benzyl Acetate (58) (Scheme 1, R = CH$_2$OAc). 5-(4-(Hydroxymethyl)phenyl)thiophene-2-carbaldehyde (**24**) (140 mg, 0.64 mmol), 2-thioxoimidazolidin-4-one (89 mg, 0.77 mmol), and β-alanine (69 mg, 0.77 mmol) were suspended in AcOH (5 mL), and the mixture was heated at reflux for 15 h. When the mixture was cooled, an orange solid crystallized out of solution which was collected by filtration and purified by flash column chromatography on silica gel (20% THF/hexanes), giving **58** as an orange solid (18%), mp (THF/n-pentane) 230–234 °C. ^{1}H NMR [400 MHz, (CD$_3$)$_2$SO] δ 12.37 (s, 1 H), 11.95 (s, 1 H), 7.83 (d, J = 4.0 Hz, 1 H), 7.72 (d, J = 8.3 Hz, 2 H), 7.65 (d, J = 4.0 Hz, 1 H), 7.44 (d, J = 8.4 Hz, 2 H), 6.63 (s, 1 H), 5.10 (s, 2 H), 2.08 (s, 3 H). LRMS (APCI$^+$) calcd for C$_{17}$H$_{15}$N$_2$O$_3$S$_2$ 359 (MH$^+$), found 359. Anal. (C$_{17}$H$_{14}$N$_2$O$_3$S$_2$) C, H, N.

General Procedure D: 4-(5-Formylthiophen-2-yl)-N-methyl-benzamide (34) (Scheme 1, R = CONR$_1$R$_2$, where NR$_1$R$_2$ = NHMe). 4-(5-Formylthiophen-2-yl)benzoic acid (**28**) (85 mg, 0.37 mmol) was dissolved in THF (5 mL), to which was added pyridine (289 mg, 3.67 mmol), followed by pentafluorophenyl trifluoroacetate (PFP-TFA). This mixture was stirred at room temperature for 15 h. Then all solvent was removed under reduced pressure to afford a crude solid which was dissolved in EtOAc (25 mL) and washed with 1 M HCl (2 × 25 mL), water (25 mL), saturated NaHCO$_3$ (25 mL), and brine (25 mL). The organic layer was then dried (Na$_2$SO$_4$), filtered and the solvent removed under reduced pressure to give the crude intermediate ester (146 mg, 0.37 mmol) which was immediately dissolved in THF (5 mL) and treated with 2 M methylamine in MeOH (1.85 mL, 3.70 mmol). After the mixture was stirred for 1 h at room temperature, 1 M HCl (5 mL) was added to hydrolyze the undesired imine. The reaction mixture was then diluted with water (20 mL) and extracted with EtOAc (2 × 20 mL). Then the combined organic fractions were dried (Na$_2$SO$_4$), filtered, and evaporated down to give a crude solid. Trituration with Et$_2$O gave **34** as a pale yellow solid (80%). ^{1}H NMR [400 MHz, (CD$_3$)$_2$SO] δ 9.93 (s, 1 H), 8.47–8.53 (br m, 1 H), 8.07 (d, J = 4.0 Hz, 1 H), 7.93 (d, J = 8.7 Hz, 2 H), 7.89 (d, J = 8.7 Hz, 2 H), 7.84 (d, J = 4.0 Hz, 1 H), 2.80 (d, J = 4.5 Hz, 3 H). LRMS (APCI$^+$) calcd for C$_{13}$H$_{12}$NO$_2$S 246 (MH$^+$), found 246.

(E,Z)-N-Methyl-4-(5-((5-oxo-2-thioxoimidazolidin-4-ylidene)methyl)thiophen-2-yl)benzamide (67) (Scheme 1, R = CONR$_1$R$_2$, where NR$_1$R$_2$ = NHMe). Reaction of **34** with 2-thiohydantoin according to general procedure C gave **67** as a dark orange solid (76%), mp (AcOH) >300 °C. ^{1}H NMR [400 MHz, (CD$_3$)$_2$SO] δ 12.37 (br s, 1 H), 11.97 (br s, 1 H), 8.47 (br q, J = 4.5 Hz, 1 H), 7.90 (d, J = 8.5 Hz, 2 H), 7.84 (d, J = 4.0 Hz, 1 H), 7.80 (d, J = 8.5 Hz, 2 H), 7.74 (d, J = 4.0 Hz, 1 H), 2.79 (d, J = 4.5 Hz, 3 H). LRMS (APCI$^−$) calcd for C$_{16}$H$_{12}$N$_3$O$_2$S$_2$ 342 (M − H), found 342. Anal. (C$_{16}$H$_{13}$N$_3$O$_2$S$_2$) C, H, N.

General Procedure E: 5-(5-(1,3-Dioxolan-2-yl)thiophen-2-yl)isoindolin-1-one (82) (Scheme 2, R$_1$ = H, R$_2$R$_3$ = Dioxolane). 2-Thiophenecarboxaldehyde was protected as the cyclic acetal according to a literature procedure.[44] 2-(Thiophen-2-yl)-1,3-dioxolane was then reacted with 5-iodoisobenzofuran-1(3H)-one (**77**) using a procedure adapted from a literature reference.[37] The iodide (1.23 g, 4.75 mmol), PdCl$_2$(PPh$_3$)$_2$ (333 mg, 0.48 mmol), and KF (1.10 g, 19.0 mmol) were weighed into a flask and dissolved in DMSO (35 mL). The

mixture was placed under an atmosphere of N$_2$. 2-(Thiophen-2-yl)-1,3-dioxolane (2.22 g, 14.2 mmol) and AgNO$_3$ (807 mg, 4.75 mmol) were added,. Then the resulting suspension was stirred for 0.5 h at 100 °C. Further portions of AgNO$_3$ (3 × 807 mg) were added at 0.5 h intervals to give a total reaction time of 2 h. Upon cooling, the mixture was filtered through a plug of Celite which was washed well with CHCl$_3$. The resulting CHCl$_3$ solution (∼200 mL) was washed with water (3 × 100 mL), dried (Na$_2$SO$_4$), filtered and the solvent removed under reduced pressure to give a crude solid which was purified by flash column chromatography on silica gel (5% acetone/CH$_2$Cl$_2$ as eluant). Trituation with Et$_2$O gave **82** as a pale yellow solid (61%). ^{1}H NMR [400 MHz, (CD$_3$)$_2$SO] δ 8.53 (br s, 1 H), 7.85 (d, J = 0.6 Hz, 1 H), 7.76 (dd, J = 7.9, 1.6 Hz, 1 H), 7.68 (d, J = 7.9 Hz, 1 H), 7.53 (d, J = 3.7 Hz, 1 H), 7.25 (d, J = 3.6 Hz, 1 H), 6.07 (s, 1 H), 4.41 (s, 2 H), 4.02–4.09 (m, 2 H), 3.94–4.01 (m, 2 H). LRMS (APCI$^+$) calcd for C$_{15}$H$_{14}$NO$_3$S 288 (MH$^+$), found 288.

General Procedure F: 5-(5-(1,3-Dioxolan-2-yl)thiophen-2-yl)-2-methylisoindolin-1-one (87) (Scheme 2, R$_1$ = Me, R$_2$R$_3$ = Dioxolane). 5-(5-(1,3-Dioxolan-2-yl)thiophen-2-yl)isoindolin-1-one (**82**) (150 mg, 0.52 mmol) was dissolved in dry DMF (10 mL), and the resulting solution was cooled to 0 °C (ice/water). NaH (23 mg, 0.58 mmol) was added and the mixture stirred for 0.5 h at this temperature. Methyl iodide (82 mg, 0.58 mmol) was added dropwise to the solution of anion and the mixture stirred for 0.25 h at 0 °C, followed by 1 h at room temperature. The mixture was diluted with water (50 mL) and extracted with EtOAc (3 × 50 mL). The combined EtOAc fractions were washed with water (3 × 50 mL), brine (50 mL) and dried (Na$_2$SO$_4$). Filtration and removal of the solvent under reduced pressure gave a crude yellow solid which was purified by flash column chromatography on silica gel (5% acetone/CH$_2$Cl$_2$ as eluant) to give **87** as a yellow solid (82%). ^{1}H NMR [400 MHz, (CD$_3$)$_2$SO] δ 7.87 (d, J = 0.7 Hz, 1 H), 7.76 (dd, J = 7.9, 1.6 Hz, 1 H), 7.67 (d, J = 8.0 Hz, 1 H), 7.53 (d, J = 3.8 Hz, 1 H), 7.25 (d, J = 3.8 Hz, 1 H), 6.07 (s, 1 H), 4.49 (s, 2 H), 4.02–4.09 (m, 2 H), 3.94–3.99 (m, 2 H), 3.08 (s, 3 H). LRMS (APCI$^+$) calcd for C$_{16}$H$_{16}$NO$_3$S 302 (MH$^+$), found 302.

5-(2-Methyl-1-oxoisoindolin-5-yl)thiophene-2-carbaldehyde (95) (Scheme 2, R$_1$ = Me, R$_5$ = H). Deprotection of **87** according to general procedure B gave **95** as a yellow solid (89%). ^{1}H NMR [400 MHz, (CD$_3$)$_2$SO] δ 9.94 (s, 1 H), 8.08 (d, J = 4.0 Hz, 1 H), 8.04 (d, J = 0.8 Hz, 1 H), 7.91 (dd, J = 7.9, 1.6 Hz, 1 H), 7.86 (d, J = 4.0 Hz, 1 H), 7.74 (d, J = 7.9 Hz, 1 H), 4.53 (s, 2 H), 3.09 (s, 3 H). LRMS (APCI$^+$) calcd for C$_{14}$H$_{12}$NO$_2$S 258 (MH$^+$), found 258.

(E,Z)-2-Methyl-5-(5-((5-oxo-2-thioxoimidazolidin-4-ylidene)methyl)thiophen-2-yl)isoindolin-1-one (119) (Scheme 2, R$_1$ = Me, R$_5$ = H). Reaction of **95** with 2-thiohydantoin according to general procedure C gave **119** as an orange solid (92%), mp (AcOH) >300 °C. ^{1}H NMR [400 MHz, (CD$_3$)$_2$SO; observe E- and Z- isomers separately)] δ 11.90–12.38 (m, 2 H), 7.92 (br d, J = 0.7 Hz, 1 H), 7.82 (br d, J = 4.0 Hz, 0.8 H), 7.80–7.84 (m, 1 H), 7.75–7.78 (m, 1 H), 7.67–7.73 (m, 1.2 H), 6.82 (s, 0.2 H), 6.65 (s, 0.8 H), 4.51 (s, 2 H), 3.09 (s, 3 H). LRMS (APCI$^−$) calcd for C$_{17}$H$_{12}$N$_3$O$_2$S$_2$ 354 (M − H), found 354.

General Procedure G: 2-(2-Hydroxyethyl)-5-iodoisoindolin-1-one (78) (Scheme 2, R$_1$ = CH$_2$CH$_2$OH). Methyl 4-iodo-2-methylbenzoate[45] (**76**) (860 mg, 3.12 mmol) was dissolved in benzene (10 mL), to which were added N-bromosuccinimide (NBS) (666 mg, 3.74 mmol) and 2,2′-azobis(2-methylpropionitrile) (51 mg, 0.31 mmol). This mixture was heated at reflux temperature for 6 h. The mixture was allowed to cool, filtered and the resulting filtrate diluted with Et$_2$O (100 mL). This solution was washed with saturated sodium metabisufite (50 mL) and brine (50 mL), dried (Na$_2$SO$_4$), and filtered. Removal of the solvent under reduced pressure gave a transparent oil which was purified by filtration through a plug of silica gel (5% EtOAc/hexanes as eluant). The resulting oil solidified under high vacuum to afford a white solid (1.08 g), shown to be 93% desired monobromide and 7% unreacted starting material by ^{1}H NMR. This solid was used directly in the next step.

The bromide (1.08 mg, 3.04 mmol) was dissolved in THF (10 mL), and 2-aminoethanol (928 mg, 15.2 mmol) was added. The reaction mixture was stirred at room temperature for 15 h. Then all solvent was removed under reduced pressure. The resulting residue was purified by

flash column chromatography on silica gel (10% acetone/CH$_2$Cl$_2$ as eluant) to give **78** as a crystalline white solid (562 mg, 59% over two steps). ^{1}H NMR [400 MHz, (CD$_3$)$_2$SO] δ 8.02 (d, J = 0.7 Hz, 1 H), 7.84 (dd, J = 7.9, 1.4 Hz, 1 H), 7.45 (d, J = 7.9 Hz, 1 H), 4.82 (t, J = 5.4 Hz, 1 H), 4.52 (s, 2 H), 3.58–3.64 (m, 2 H), 3.32–3.57 (m, 2 H). LRMS (APCI$^+$) calcd for C$_{10}$H$_{11}$INO$_2$ 304 (MH$^+$), found 304.

General Procedure H: 5-(2-(2-Hydroxyethyl)-1-oxoisoindolin-5-yl)thiophene-2-carbaldehyde (100) (Scheme 2, R$_1$ = CH$_2$CH$_2$OH, R$_5$ = H). 2-Thiophenecarboxaldehyde was protected as the dimethyl acetal according to a literature procedure,[46] then reacted with **78** according to general procedure E to give **83**. Deprotection directly to the aldehyde was then carried out as follows. Compound **83** (430 mg, 1.29 mmol) was dissolved in acetone (32 mL), to which were added water (8 mL) and p-toluenesulfonic acid (100 mg). This mixture was stirred at 50 °C for 5 h. Upon cooling, the reaction mixture was diluted with water (100 mL) and extracted with CH$_2$Cl$_2$ (3 × 50 mL). Purification by flash column chromatography on silica gel (5% MeOH/CH$_2$Cl$_2$ as eluant) gave **100** as a yellow solid (378 mg, 71% over two steps). ^{1}H NMR [400 MHz, (CD$_3$)$_2$SO] δ 9.94 (s, 1 H), 8.08 (d, J = 4.0 Hz, 1 H), 8.04 (d, J = 0.8 Hz, 1 H), 7.92 (dd, J = 7.9, 1.6 Hz, 1 H), 7.85 (d, J = 4.0 Hz, 1 H), 7.75 (d, J = 8.0 Hz, 1 H), 4.83 (t, J = 5.4 Hz, 1 H), 4.62 (s, 2 H), 3.56–3.67 (m, 4 H). LRMS (APCI$^+$) calcd for C$_{15}$H$_{14}$NO$_3$S 288 (MH$^+$), found 288.

(E,Z)-2-(1-Oxo-5-(5-((5-oxo-2-thioxoimidazolidin-4-ylidene)methyl)thiophen-2-yl)isoindolin-2-yl)ethyl Acetate (124) (Scheme 2, R$_1$ = CH$_2$CH$_2$OAc, R$_5$ = H). Reaction of **100** with 2-thiohydantoin according to general procedure C gave **124** as a red powder (57%), mp (AcOH) 261–264 °C. ^{1}H NMR [400 MHz, (CD$_3$)$_2$SO] δ 12.39 (s, 1 H), 11.98 (s, 1 H), 7.92–7.96 (m, 1 H), 7.87 (d, J = 4.0 Hz, 1 H), 7.84 (dd, J = 8.0, 1.5 Hz, 1 H), 7.77 (d, J = 4.0 Hz, 1 H), 7.73 (d, J = 7.9 Hz, 1 H), 6.65 (s, 1 H), 4.59 (s, 2 H), 4.26 (t, J = 5.4, Hz, 2 H), 3.78 (t, J = 5.3, Hz, 2 H), 2.00 (s, 3 H).

General Procedure I: (E,Z)-2-(2-Hydroxyethyl)-5-(5-((5-oxo-2-thioxoimidazolidin-4-ylidene)methyl)thiophen-2-yl)-isoindolin-1-one (125) (Scheme 2, R$_1$ = CH$_2$CH$_2$OH, R$_5$ = H). Hydrolysis of **124** (161 mg, 0.42 mmol) was carried out by removing the previous reaction solvent (AcOH, 4 mL) from the reaction mixture under reduced pressure and treating the crude O-acetate with K$_2$CO$_3$ (289 mg, 2.09 mmol) in a mixture of MeOH (10 mL) and water (2 mL) at room temperature for 1 h. The MeOH was removed under reduced pressure to give an orange-black oil which was cooled to 0 °C (ice/water) and acidified with 1 M HCl. The resulting solid was collected by filtration, allowed to air-dry, then stirred in warm MeOH until a homogeneous suspension was obtained. This was collected by filtration and dried under vacuum to give **125** as an orange solid (78 mg, 48% over two steps), mp (AcOH) 285 °C (dec). ^{1}H NMR [400 MHz, (CD$_3$)$_2$SO; observe E- and Z- isomers separately] δ 11.98–12.39 (m, 2 H), 7.93 (br s, 1 H), 7.87 (d, J = 4.0 Hz, 1 H), 7.83 (dd, J = 8.0, 1.5 Hz, 0.9 H), 7.77 (d, J = 4.0 Hz, 1 H), 7.72 (d, J = 8.0 Hz, 1 H), 7.68 (d, J = 4.0 Hz, 0.1 H), 6.84 (s, 0.1 H), 6.65 (s, 0.9 H), 4.82 (t, J = 5.2 Hz, 1 H), 4.60 (s, 2 H), 3.62–3.67 (m, 2 H), 3.56–3.61 (m, 2 H). LRMS (APCI$^-$) calcd for C$_{18}$H$_{14}$N$_3$O$_3$S$_2$ 384 (M − H), found 384.

General Procedure J: (E,Z)-2-(2-Morpholinoethyl)-5-(5-((5-oxo-2-thioxoimidazolidin-4-ylidene)methyl)thiophen-2-yl)-isoindolin-1-one (130) (Scheme 2, R$_1$ = CH$_2$CH$_2$morpholine, R$_5$ = H). Reaction of **105** with 2-thiohydantoin according to general procedure C gave **130**. In this case (and others where the target compound contained an amine) the AcOH solvent was removed under reduced pressure to afford an orange-black oil which gave an orange solid when suspended and stirred in a mixture of acetone (5 mL) and saturated NaHCO$_3$ (10 mL). This solid was collected by filtration, dried under vacuum, and triturated with MeOH to afford **130** as an orange solid (72%), mp (MeOH) 261–264 °C. ^{1}H NMR [400 MHz, (CD$_3$)$_2$SO; observe E- and Z- isomers separately] δ 11.97–12.29 (m, 2 H), 7.94 (s, 1 H), 7.80–7.87 (m, 2 H), 7.75–7.79 (m, 1 H), 7.72 (d, J = 8.0 Hz, 0.85 H), 7.68 (d, J = 3.9 Hz, 0.15 H), 6.84 (s, 0.15 H), 6.64 (s, 0.15 H), 4.61 (s, 2 H), 3.66 (t, J = 6.2 Hz, 2 H), 3.55 (t, J = 4.5 Hz, 4 H), 2.57 (t, J = 6.2 Hz, 2 H), 2.43 (br s, 4 H). LRMS (APCI$^+$) calcd for C$_{22}$H$_{23}$N$_4$O$_3$S$_2$ 455 (M + H), found 455. HRMS (ESI$^+$) calcd for C$_{22}$H$_{23}$N$_4$O$_3$S$_2$ 455.1206 (MH$^+$), found 455.1201.

5-(5-(Dimethoxymethyl)thiophen-2-yl)-2-(3-hydroxypropyl)-isoindolin-1-one (107) (Scheme 2, R$_4$ = OH). Compound **101** (1.20 g, 3.98 mmol) was dissolved in a mixture of MeOH (50 mL) and trimethyl orthoformate (5 mL). p-Toluenesulfonic acid (100 mg) was added, along with 4 Å molecular sieves (5.0 g). Then the reaction mixture was heated at reflux for 15 h. Upon cooling, the reaction mixture was diluted with CH$_2$Cl$_2$ (100 mL) and filtered through Celite which was washed well with CH$_2$Cl$_2$. The solvent was removed from the combined filtrate under reduced pressure to give an oil which was dissolved in EtOAc (150 mL) and washed with saturated NaHCO$_3$ (2 × 100 mL), water (100 mL), and brine (100 mL). The organic phase was dried (Na$_2$SO$_4$), filtered and the solvent removed to afford **107** as a waxy, pale yellow solid (100%). ^{1}H NMR [400 MHz, (CD$_3$)$_2$SO] δ 7.86 (d, J = 0.8 Hz, 1 H), 7.75 (dd, J = 8.0, 1.5 Hz, 1 H), 7.67 (d, J = 7.9 Hz, 1 H), 7.54 (d, J = 3.7 Hz, 1 H), 7.02 (dd, J = 3.8, 0.8 Hz, 1 H), 5.66 (d, J = 0.7 Hz, 1 H), 4.51 (s, 2 H), 4.49 (t, J = 5.1 Hz, 1 H), 3.57 (t, J = 7.2 Hz, 2 H), 3.45 (q, J = 5.9 Hz, 2 H), 3.32 (s, 6 H), 1.76 (pentet, J = 6.7 Hz, 2 H). LRMS (APCI$^+$) calcd for C$_{18}$H$_{22}$NO$_4$S 348 (MH$^+$), found 348.

3-(5-(5-(Dimethoxymethyl)thiophen-2-yl)-1-oxoisoindolin-2-yl)propyl Methanesulfonate (108) (Scheme 2, R$_4$ = OMs). Alcohol **107** (1.29 g, 3.72 mmol) was dissolved in dry THF (40 mL). Triethylamine (3.76 g, 37.2 mmol) and methanesulfonyl chloride (1.70 g, 14.9 mmol) were added, and the reaction mixture was stirred at room temperature for 3.5 h. The mixture was diluted with EtOAc (200 mL), which was washed with water (100 mL), saturated NaHCO$_3$ (100 mL), and brine (100 mL). The organic layer was dried (Na$_2$SO$_4$), filtered and the solvent removed under reduced pressure to give a residue which was purified by flash column chromatography on silica gel (5% acetone/CH$_2$Cl$_2$ as eluant), giving **108** as a waxy yellow solid (1.58 g, 100%). ^{1}H NMR [400 MHz, (CD$_3$)$_2$SO] δ 7.87 (d, J = 0.7 Hz, 1 H), 7.76 (dd, J = 7.9, 1.5 Hz, 1 H), 7.69 (d, J = 7.6 Hz, 1 H), 7.55 (d, J = 3.7 Hz, 1 H), 7.12 (dd, J = 3.7, 0.8 Hz, 1 H), 5.66 (d, J = 0.6 Hz, 1 H), 4.53 (s, 2 H), 4.25 (t, J = 6.2 Hz, 2 H), 3.63 (t, J = 6.9 Hz, 2 H), 3.32 (s, 6 H), 3.18 (s, 3 H), 2.04 (pentet, J = 6.6 Hz, 2 H). LRMS (APCI$^+$) calcd for C$_{19}$H$_{24}$NO$_6$S$_2$ 426 (MH$^+$), found 426.

5-(5-(Dimethoxymethyl)thiophen-2-yl)-2-(3-iodopropyl)-isoindolin-1-one (109) (Scheme 2, R$_4$ = I). Mesylate **108** (624 mg, 1.47 mmol) was dissolved in acetone (30 mL) at 70 °C. Then NaI (4.40 g, 29.3 mmol) was added. Stirring was continued at this temperature for 1 h. Then the mixture was allowed to cool and was filtered through Celite which was washed well with acetone. The solvent was removed from the combined filtrate under reduced pressure to give a residue which was purified by flash column chromatography on silica gel (10% acetone/CH$_2$Cl$_2$ as eluant), giving **109** as a waxy yellow solid (660 mg, 96%). ^{1}H NMR [400 MHz, (CD$_3$)$_2$SO] δ 7.86 (d, J = 0.8 Hz, 1 H), 7.76 (dd, J = 7.9, 1.6 Hz, 1 H), 7.68 (d, J = 7.9 Hz, 1 H), 7.55 (d, J = 3.7 Hz, 1 H), 7.12 (dd, J = 3.7, 0.8 Hz, 1 H), 5.66 (d, J = 0.7 Hz, 1 H), 4.53 (s, 2 H), 3.58 (t, J = 6.9 Hz, 2 H), 3.32 (s, 6 H), 3.25 (t, J = 6.9 Hz, 2 H), 2.14 (pentet, J = 6.9 Hz, 2 H). LRMS (APCI$^+$) calcd for C$_{18}$H$_{21}$INO$_3$S 458 (MH$^+$), found 458.

General Procedure K: 5-(2-(3-(Dimethylamino)propyl)-1-oxoisoindolin-5-yl)thiophene-2-carbaldehyde (114) (Scheme 2, R$_1$ = (CH$_2$)$_3$NMe$_2$, R$_5$ = H). Iodide **109** (330 mg, 0.71 mmol) was dissolved in dimethylacetamide (10 mL), to which was added dimethylamine (3.53 mL of a 2 M solution in THF), and the resulting mixture was stirred for 15 h at room temperature. All solvent was removed under reduced pressure to give a viscous oil which was dissolved in EtOAc (100 mL). This solution was washed with water (3 × 100 mL), brine (100 mL) and dried (Na$_2$SO$_4$). Filtration and removal of the solvent under reduced pressure gave the crude dimethyl acetal protected product (**110**) as a yellow oil. This product was then deprotected directly to the desired aldehyde according to general procedure H. Trituration with Et$_2$O gave **114** as a yellow solid (140 mg, 60%). ^{1}H NMR [400 MHz, (CD$_3$)$_2$SO] δ 9.94 (s, 1 H), 8.08 (d, J = 4.0 Hz, 1 H), 8.03 (d, J = 0.7 Hz, 1 H), 7.92 (dd, J = 8.0, 1.6 Hz, 1 H), 7.86 (d, J = 4.0 Hz, 1 H), 7.75 (d, J = 7.9 Hz, 1 H), 4.55 (s, 2 H), 3.56 (t, J = 7.2 Hz, 2 H), 2.24 (t, J = 7.1 Hz, 2 H), 2.13 (s, 6 H), 1.74 (pentet, J = 7.2 Hz, 2 H). LRMS (APCI$^+$) calcd for C$_{18}$H$_{21}$N$_2$O$_2$S 329 (MH$^+$), found 329.

(E,Z)-2-(3-(Dimethylamino)propyl)-5-(5-((5-oxo-2-thioxoimidazolidin-4-ylidene)methyl)thiophen-2-yl)isoindolin-1-one

(131) (Scheme 2, R$_1$ = (CH$_2$)$_3$NMe$_2$, R$_5$ = H). Reaction of **114** with 2-thiohydantoin according to general procedure C, followed by isolation according to general procedure J, gave **131** as a dark orange solid (51%), mp (MeOH) 212 °C (dec). ^{1}H NMR [400 MHz, (CD$_3$)$_2$SO] δ 11.47 (v br s, 2 H), 7.91 (br s, 1 H), 7.82 (dd, J = 8.0, 1.4 Hz, 1 H), 7.67−7.73 (m, 3 H), 6.52 (s, 1 H), 4.53 (s, 2 H), 3.56 (t, J = 7.0 Hz, 2 H), 2.40−2.47 (m, 2 H), 2.33 (s, 6 H), 1.81 (pentet, J = 7.2 Hz, 2 H). LRMS (APCI$^+$) calcd for C$_{21}$H$_{23}$N$_4$O$_2$S$_2$ 427 (MH$^+$), found 427.

5-(5-(1,3-Dioxolan-2-yl)thiophen-2-yl)-2,3-dimethylisoindolin-1-one (93). Compound **87** was dissolved in dry THF (10 mL) and cooled to −78 °C under N$_2$. Lithium diisopropylamide in cyclohexane (0.40 mL of a 1.5 M solution, 0.59 mmol) was added dropwise. Then the mixture was stirred for a further 0.25 h at this temperature. Methyl iodide (84 mg, 0.59 mmol) was added dropwise with stirring continued at −78 °C for 0.5 h, at which point the mixture was allowed to warm to room temperature. The mixture was diluted with saturated NH$_4$Cl (50 mL) and extracted with EtOAc (3 × 50 mL). The combined EtOAc fractions were washed with brine (50 mL) and dried (Na$_2$SO$_4$). Filtration and removal of the solvent under reduced pressure gave a brown oil which was purified by flash column chromatography on silica gel (5% acetone/CH$_2$Cl$_2$ as eluant) to give **93** as a yellow oil (65%). ^{1}H NMR [400 MHz, (CD$_3$)$_2$SO] δ 7.92 (t, J = 0.7 Hz, 1 H), 7.75 (dd, J = 7.9, 1.4 Hz, 1 H), 7.66 (d, J = 7.9 Hz, 1 H), 7.55 (d, J = 3.7 Hz, 1 H), 7.26 (d, J = 3.7 Hz, 1 H), 6.07 (s, 1 H), 4.59 (q, J = 6.7 Hz, 1 H), 4.02−4.09 (m, 2 H), 3.94−4.02 (m, 2 H), 3.01 (s, 3 H), 1.47 (d, J = 6.7 Hz, 3 H). LRMS (APCI$^+$) calcd for C$_{17}$H$_{18}$NO$_3$S 316 (M + H), found 316.

5-(2,3-Dimethyl-1-oxoisoindolin-5-yl)thiophene-2-carbaldehyde (106) (Scheme 2, R$_1$ = Me, R$_5$ = Me). Deprotection of **93** was carried out according to general procedure B to give **106** as a beige solid (96%). ^{1}H NMR [400 MHz, (CD$_3$)$_2$SO] δ 9.94 (s, 1 H), 8.07−8.10 (m, 2 H), 7.91 (dd, J = 8.0, 1.4 Hz, 1 H), 7.88 (d, J = 4.0 Hz, 1 H), 7.73 (d, J = 7.9 Hz, 1 H), 4.63 (q, J = 6.7 Hz, 1 H), 3.02 (s, 3 H), 1.49 (d, J = 6.7 Hz, 3 H). LRMS (APCI$^+$) calcd for C$_{15}$H$_{14}$NO$_2$S 272 (M + H), found 272.

(E,Z)-2,3-Dimethyl-5-(5-((5-oxo-2-thioxoimidazolidin-4-ylidene)methyl)thiophen-2-yl)isoindolin-1-one (135) (Scheme 2, R$_1$ = Me, R$_5$ = Me). Reaction of **106** with 2-thiohydantoin according to general procedure C gave **135** as an orange solid (57%), mp (AcOH) 286 °C (dec). ^{1}H NMR [400 MHz, (CD$_3$)$_2$SO; observe E- and Z-isomers separately] δ 11.92−12.38 (m, 2 H), 7.95−7.99 (m, 1 H), 7.87 (d, J = 4.0 Hz, 0.75 H), 7.72−7.82 (m, 2 H), 7.68−7.72 (m, 1.25 H), 6.84 (s, 0.25 H), 6.64 (s, 0.75 H), 4.61 (q, J = 6.7 Hz, 1 H), 3.02 (s, 3 H), 1.48 (d, J = 6.7 Hz, 3 H). HRMS (ESI$^-$) calcd for C$_{18}$H$_{14}$N$_3$O$_2$S$_2$ 368.0533 (M − H), found 368.0526.

6-Bromo-2-methylisoindolin-1-one (138). 6-Bromoisoindolin-1-one (**137**) was alkylated with methyl iodide and NaH according to general procedure F to give **138** as a pale yellow solid (68%). ^{1}H NMR [400 MHz, (CD$_3$)$_2$SO] δ 7.74−7.79 (m, 2 H), 7.56 (dd, J = 7.9, 0.7 Hz, 1 H), 4.44 (s, 2 H), 3.07 (s, 3 H). LRMS (APCI$^+$) calcd for C$_9$H$_9$BrNO 226, 228 (MH$^+$), found 226, 228.

General Procedure L: 2-Methyl-6-(4,4,5,5-tetramethyl-1,3,2-dioxaborolan-2-yl)isoindolin-1-one (148). 6-Bromo-2-methylisoindolin-1-one (**138**) (723 mg, 3.41 mmol), bis(pinacolato)diboron (1.04 g, 4.09 mmol), potassium acetate (1.00 g, 10.2 mmol), and Pd(dppf)Cl$_2$ catalyst (139 mg, 0.17 mmol) were weighed into a flask that was sealed under N$_2$. DMSO (15 mL) was added, and the entire mixture was stirred at 90 °C for 5 h. Upon cooling, the reaction mixture was diluted with water (250 mL) and extracted with CH$_2$Cl$_2$ (5 × 50 mL). The combined CH$_2$Cl$_2$ fractions were in turn washed with water (2 × 100 mL), brine (100 mL), dried (Na$_2$SO$_4$), filtered and the solvent was removed under reduced pressure to yield the crude product. Purification was carried out by flash column chromatography on silica gel (20% THF/CH$_2$Cl$_2$ as eluant) to give **148** as a crystalline beige solid (262 mg, 28%). ^{1}H NMR [400 MHz, (CD$_3$)$_2$SO] δ 7.91 (br s, 1 H), 7.85 (dd, J = 7.6, 1.0 Hz, 1 H), 7.59 (dd, J = 7.5, 0.6 Hz, 1 H), 4.49 (s, 2 H), 3.07 (s, 3 H), 1.32 (s, 12 H). LRMS (APCI$^+$) calcd for C$_{15}$H$_{21}$BNO$_3$ 274 (MH$^+$), found 274.

5-(2-Methyl-3-oxoisoindolin-5-yl)thiophene-2-carbaldehyde (160). Reaction of **148** with 2-(5-bromothiophen-2-yl)-1,3-dioxolane (**5**) according to general procedure A followed by deprotection of **154** directly to the aldehyde according to general procedure B gave **160** as a

pale yellow solid (91%). ^{1}H NMR [400 MHz, (CD$_3$)$_2$SO] δ 9.93 (s, 1 H), 8.06 (d, J = 4.0 Hz, 1 H), 7.99−8.03 (m, 2 H), 7.88 (d, J = 4.0 Hz, 1 H), 7.70 (dd, J = 7.8, 0.8 Hz, 1 H), 4.52 (s, 2 H), 3.10 (s, 3 H). LRMS (APCI$^+$) calcd for C$_{14}$H$_{12}$NO$_2$S 258 (MH$^+$), found 258.

(E,Z)-2-Methyl-6-(5-((5-oxo-2-thioxoimidazolidin-4-ylidene)methyl)thiophen-2-yl)isoindolin-1-one (166). Reaction of **160** with 2-thiohydantoin according to general procedure C gave **166** as an orange solid (89%), mp (AcOH) >310 °C. ^{1}H NMR [400 MHz, (CD$_3$)$_2$SO; observe E- and Z-isomers separately] δ 11.97−12.34 (m, 2 H), 7.91−7.96 (m, 2 H), 7.82 (d, J = 4.0 Hz, 0.85 H), 7.75−7.78 (m, 1 H), 7.69 (d, J = 4.0 Hz, 0.15 H), 7.66 (d, J = 8.6 Hz, 1 H), 6.84 (s, 0.15 H), 6.66 (s, 0.85 H), 4.40 (s, 2 H), 3.10 (s, 3 H). LRMS (APCI$^-$) calcd for C$_{17}$H$_{12}$N$_3$O$_3$S$_2$ 354 (M − H), found 354.

Inhibition of Perforin Mediated Lysis of Sheep Red Blood Cells (SRBC). As reported previously,[26] compound **3** was identified from screening a commercial library of ∼100 000 compounds for the ability to reproducibly inhibit perforin-mediated lysis of SRBC at a compound concentration of 100 μM.

Inhibition of Perforin-Mediated Lysis of Jurkat Cells. The ability of the compounds to inhibit the lysis of nucleated (Jurkat T lymphoma) cells in the presence of 0.1% BSA was measured by release of ^{51}Cr label. Jurkat target cells were labeled by incubation in medium with 100 μCi ^{51}Cr for 1 h. The cells were then washed three times to remove unincorporated isotope and resuspended at 1 × 10^5 cells per milliliter in RPMI buffer supplemented with 0.1% BSA. Each test compound was preincubated to concentrations of 20, 10, 5, 2.5, and 1.25 μM with recombinant perforin for 30 min with DMSO as a negative control. ^{51}Cr labeled Jurkat cells were then added, and the cells were incubated at 37 °C for 4 h. The supernatant was collected and assessed for its radioactive content on a γ counter (Wallac Wizard 1470 automatic γ counter). Each data point was performed in triplicate, and an IC$_{50}$ was calculated from the range of concentrations described above. Compounds with IC$_{50}$ < 1 μM were titrated to lower concentrations in the same manner as above, to determine an accurate IC$_{50}$.

KHYG-1 Cytotoxicity Assay. KHYG-1 cells were washed and resuspended in RPMI + 0.1% BSA at 4 × 10^5 cells/mL, and an amount of 50 μL of KHYG-1 cells was dispensed to each well of a 96-well V-bottom plate. RPMI (50 μL) + 0.1% BSA or 10% (final concentration) of serum was added to each well. Then test compounds were added to KHYG-1 cells at various concentrations up to 20 μM and incubated at room temperature for 20 min. 1 × 10^6 K562 target cells were labeled with 75 μCi ^{51}Cr in 200 μL of RPMI for 90 min at 37 °C. Cells were washed as described above and resuspended in 5 mL of RPMI + 0.1% BSA. An amount of 50 μL of ^{51}Cr labeled K562 leukemia target cells was added to each well of the KHYG-1 plate (effector/target 2:1) and incubated at 37 °C for 4 h. ^{51}Cr release was assayed using a Skatron harvesting press and radioactivity estimated on a Wallac Wizard 1470 automatic γ counter (Turku, Finland). The percentage of specific cytotoxicity was calculated using the following formula:

$$\% \text{ specific lysis} = \frac{\text{experimental release} - \text{spontaneous release}}{\text{maximum release} - \text{spontaneous release}} \times 100$$

and expressed as the mean of triplicate assays ± standard error of the mean.

Toxicity to KHYG-1 NK Cells. The toxicity assay was carried out in exactly the same manner as the killing assay above, but instead of adding the labeled K562 target cells, 100 μL of RPMI 0.1% BSA was added. Cells were incubated for 4 h at 37 °C and then washed ×3 in RPMI + 0.1% BSA. Cells were then resuspended in 200 μL of complete medium and incubated for 18−24 h at 37 °C. Trypan blue was added to each well. Viable (clear) cells and total (clear + blue) cells were counted, and the percentage of viable cells was calculated compared to DMSO treated cell control (% viability).

Plasma Pharmacokinetics and MTD Determinations. Pharmacokinetic studies were carried out in healthy CD-1 male mice (n = 3 at each time point) using intravenous administration of **135** and **167** at a concentration of 5 mg/kg in 20% 2-hydroxypropyl-β-cyclodextrin (Sigma-Aldrich). Blood was collected by cardiac puncture at 5 and 30

min and 1, 2, 4, and 6 h postdose in ice-cold $K_{2\text{-EDTA}}$ tubes. Plasma samples were separated by centrifuging at $4000g$ for 8 min and stored at $-80\ ^\circ$C until analysis. Frozen plasma was thawed on wet ice on the day of analysis. Then the sample (10 μL) was transferred to a clean microcentrifuge tube and mixed with three volumes of ice-cold acetonitrile/methanol (3:1 v/v) [containing **213** as internal standard (Table 6, Supporting Information)] to precipitate the plasma proteins. The tubes were centrifuged at $15000g$ for 10 min to obtain the clear supernatant which was mixed with 0.01% formic acid–water (1:1), and concentration of the parent drug was measured through injection of 10–20 μL into an LC–MS/MS (Agilent 6410 series triple quadrupole mass spectrometry detector system). A Zorbax SB-C18, 50 mm × 2.1 mm 5 μm column was used at a 0.5 mL/min flow rate, and elution was with a gradient of organic phase (A), acetonitrile in water (80:20 v/v) containing 0.01% formic acid and aqueous phase (B), water containing 0.01% formic acid. LC–MS/MS analysis was carried out using multiple reaction monitoring. Parent drug was quantified against a standard curve 0–250 ng/mL in control mouse plasma. Plasma samples from 5 min, 30 min, and 1 h were diluted with control mouse plasma (1:20 for 5 min, 1:10 for 30 min and 1 h samples) to fit within this range. The resultant concentration vs time data were fitted (using Phoenix WinNonlin 6.2; Pharsight Corporation, St. Louis, MO) to calculate pharmacokinetic parameters including half-life ($T_{1/2}$), maximum concentration ($C_{\max}$), area under the curve ($AUC_{0-\infty}$), volume of distribution (V), and clearance (Cl).

The MTD was determined by single dose or b.i.d. × 3 intraperitoneal administration through a classical dose escalation design in C57BL/6 mice and defined as a dose level that was tolerated by mice ($n = 2-3$ mice/group) with a body weight loss of <10% and no death or detectable sickness. Mice were observed for four days postdose. All animal experiments were approved by the Animal Ethics Committee of the University of Auckland.

Measurement of Inhibitor Binding by SPR. Binding experiments with surface immobilized wild-type perforin monomers on a S-series CM5 sensor chip (GE Healthcare Life Sciences) were carried out using a Biacore T200 SPR machine (GE Healthcare Life Sciences). Perforin monomer solution (25 μg/mL in 10 mM sodium acetate, pH 5.5) was injected over the sensor chip surface under standard amide coupling conditions to obtain covalent binding of the protein (density = 4257 RU). The initial and running buffers were made from a 10× stock solution of HEPES buffered saline (HBS). 10× HBS (50 mL) was diluted to 500 mL with water and filtered through a 0.22 μm filter (initial buffer). This initial buffer (380 mL) was added to DMSO (20 mL) to prepare the 5% DMSO running buffer. Stock solutions (2.5 mM) of compound were prepared in 100% DMSO. These solutions were diluted in HEPES initial buffer to 5% DMSO (125 μM) and then subsequently diluted to the required concentrations using HEPES running buffer containing 5% DMSO to maintain a constant DMSO concentration. A solvent correction was run before and after the injections to account for differences in DMSO concentrations between buffer and analyte solutions.

Analysis of the Cytotoxic Immunological Synapse. Time-lapse microscopy and image analysis were performed as described previously.[42] In brief, primary human natural killer cells were isolated from the peripheral blood of four unrelated donors using negative selection, as described in the above reference. Natural killer cells were labeled with 1 μM Fluo-4AM for 20 min at 37 $^\circ$C/5% CO_2, and then cells were washed and preincubated for 10 min in RPMI culture medium containing 0.2% (v/v) DMSO or 20 μM **167**/0.2% (v/v) DMSO at room temperature before combining with HeLa cell targets preseeded in chamber slides. The final mixture contained complete RPMI-1640 culture medium[42] supplemented with 100 μM propidium iodide, 0.2% (v/v) DMSO or 20 μM **167**/0.2% (v/v) DMSO. All experiments were performed at 37 $^\circ$C/5% CO_2.

ASSOCIATED CONTENT

Ⓢ Supporting Information

Tables of all compounds numbered individually, selected figures, experimental, SPR, NMR, HRMS, HPLC, biological data (as

indicated in the text), and combustion analysis results of all final compounds. This material is available free of charge via the Internet at http://pubs.acs.org.

AUTHOR INFORMATION

Corresponding Author

*Phone: +64 9 3737599. Fax: +64 9 3737502. E-mail: j.spicer@auckland.ac.nz.

Notes

The authors declare no competing financial interest.

ACKNOWLEDGMENTS

ABBREVIATIONS USED

NK, natural killer; CTL, cytotoxic T lymphocyte; MACPF, membrane attack complex/perforin; EGF, epidermal growth factor; FLH, familial hemophagocytic lymphohistiocytosis; SPR, surface plasmon resonance

REFERENCES

(1) Lopez, J. A.; Brennan, A. J.; Whisstock, J. C; Voskoboinik, I.; Trapani, J. A. Protecting a serial killer: pathways for perforin trafficking and self-defence ensure sequential target cell death. *Trends Immunol.* **2012**, *33*, 406–412.

(2) de Saint Basile, G.; Ménasché, G.; Fischer, A. Molecular mechanisms of biogenesis and exocytosis of cytotoxic granules. *Nat. Rev. Immunol.* **2010**, *10*, 568–579.

(3) Hoves, S.; Trapani, J. A.; Voskoboinik, I. The battlefield of perforin/granzyme cell death pathways. *J. Leukocyte Biol.* **2010**, *87*, 237–243.

(4) Lichtenheld, M. G.; Olsen, K. J.; Lu, P.; Lowrey, D. M.; Hameed, A.; Hengartner, H.; Podack, E. R. Structure and function of human perforin. *Nature* **1988**, *335*, 448–451.

(5) Podack, E. R. Perforin: structure, function and regulation. *Curr. Top. Microbiol. Immunol.* **1992**, *178*, 175–185.

(6) Trapani, J. A.; Smyth, M. J. Functional significance of the perforin/granzyme cell death pathway. *Nat. Rev. Immunol.* **2002**, *2*, 735–747.

(7) Brennan, A. J.; Chia, J.; Browne, K. A.; Ciccone, A.; Ellis, S.; Lopez, J. A.; Susanto, O.; Verschoor, S.; Yagita, H.; Whisstock, J. C.; Trapani, J. A.; Voskoboinik, I. Protection from endogenous perforin: glycans and the C terminus regulate exocytic trafficking in cytotoxic lymphocytes. *Immunity* **2011**, *34*, 879–892.

(8) Law, R. H. P.; Lukoyanova, N.; Voskoboinik, I.; Caradoc-Davies, T. T.; Baran, K.; Dunstone, M. A.; D'Angelo, M. E.; Orlova, E. V.; Coulibaly, F.; Verschoor, S.; Browne, K. A.; Ciccone, A.; Kuiper, M. J.; Bird, P. I.; Trapani, J. A.; Saibil, H. R.; Whisstock, J. C. The structural basis for membrane binding and pore formation by lymphocyte perforin. *Nature* **2010**, *468* (7322), 447–451.

(9) Rosado, C. J.; Buckle, A. M.; Law, R. H. P.; Butcher, R. E.; Kan, W.–T.; Bird, C. H.; Ung, K.; Browne, K. A.; Baran, K.; Bashtannyk-Puhalovich, T. A.; Faux, N. G.; Wong, W.; Porter, C. J.; Pike, R. N.; Ellisdon, A. M.; Pearce, M. C.; Bottomley, S. P.; Emsley, J.; Smith, A. I.; Rossjohn, J.; Hartland, E. L.; Voskoboinik, I.; Trapani, J. A.; Bird, P. I.; Dunstone, M. A.; Whisstock, J. C. A common fold mediates vertebrate defence and bacterial attack. *Science* **2007**, *317*, 1548–1551.

(10) Baran, K.; Dunstone, M.; Chia, J.; Ciccone, A.; Browne, K. A.; Clarke, C. J. P.; Lukoyanova, N.; Saibil, H.; Whisstock, J. C.; Voskoboinik, I.; Trapani, J. A. The molecular basis for perforin oligomerization and transmembrane pore assembly. *Immunity* **2009**, *30*, 684−695.

(11) Kagi, D.; Odermatt, B.; Seiler, P.; Zinkernagel, R. M.; Mak, T. W.; Hengartner, H. Reduced incidence and delayed onset of diabetes in perforin-deficient nonobese diabetic mice. *J. Exp. Med.* **1997**, *186*, 989−997.

(12) Smyth, M. J.; Thia, K. Y. T.; Street, S. E. A.; MacGregor, D.; Godfrey, D. I.; Trapani, J. A. Perforin-mediated cytotoxicity is critical for surveillance of spontaneous lymphoma. *J. Exp. Med.* **2000**, *192*, 755−760.

(13) Stepp, S. E.; Dufourcq-Lagelouse, R.; Le Deist, F.; Bhawan, S.; Certain, S.; Mathew, P. A.; Henter, J.-I.; Bennett, M.; Fischer, A.; de Saint Basile, G.; Kumar, V. Perforin gene defects in familial hemophagocytic lymphohistiocytosis. *Science* **1999**, *286*, 1957−1959.

(14) Janka, G. E. Familial and acquired hemophagocytic lymphohistiocytosis. *Annu. Rev. Med.* **2012**, *63*, 233−246.

(15) Pearl-Yafe, M.; Kaminitz, A.; Yolcu, E. S.; Yaniv, I.; Stein, J.; Askenasy, N. Pancreatic islets under attack: cellular and molecular effectors. *Curr. Pharm. Des.* **2007**, *13*, 749−760.

(16) Thomas, H. E.; Trapani, J. A.; Kay, T. W. H. The role of perforin and granzymes in diabetes. *Cell Death Differ.* **2010**, *17*, 577−585.

(17) Voskoboinik, I.; Dunstone, M. A.; Baran, K.; Whisstock, J. C.; Trapani, J. A. Perforin: structure, function and role in human immunopathology. *Immunol. Rev.* **2010**, *235*, 35−54.

(18) Veale, J. L.; Liang, L. W.; Zhang, Q.; Gjertson, D. W.; Du, Z.; Bloomquist, E. W.; Jia, J.; Qian, L.; Wilkinson, A. H.; Danovitch, G. M.; Pham, P.-T. T.; Rosenthal, J. T.; Lassman, C. R.; Braun, J.; Reed, E. F.; Gritsch, H. A. Noninvasive diagnosis of cellular and antibody-mediated rejection by perforin and granzyme B in renal allografts. *Hum. Immunol.* **2006**, *67*, 777−786.

(19) Choy, J. C.; Kerjner, A.; Wong, B. W.; McManus, B. M.; Granville, D. J. Perforin mediates endothelial cell death and resultant transplant vascular disease in cardiac allografts. *Am. J. Pathol.* **2004**, *165*, 127−133.

(20) Barry, M.; Bleackley, R. C. Cytotoxic T lymphocytes: All roads lead to death. *Nat. Rev. Immunol.* **2002**, *2*, 401−409.

(21) Tredger, J. M.; Brown, N. W.; Dawhan, A. Immunosuppression in pediatric solid organ transplantation: opportunities, risks, and management. *Pediatr. Transplant.* **2006**, *10*, 879−892.

(22) Fantini, M. C.; Becker, C.; Kiesslich, R.; Nuerath, M. F. Drug insight: novel small molecules and drugs for immunosuppression. *Nat. Clin. Pract. Gastroenterol. Hepatol.* **2006**, *3*, 633−644.

(23) Lena, G.; Trapani, J. A.; Sutton, V. R.; Ciccone, A.; Browne, K. A.; Smyth, M. J.; Denny, W. A.; Spicer, J. A. Dihydro[3,4-c]pyridinones as inhibitors of the cytolytic effects of the pore-forming glycoprotein perforin. *J. Med. Chem.* **2008**, *51*, 7614−7624.

(24) Lyons, D. M.; Huttunen, K. M.; Browne, K. A.; Ciccone, A.; Trapani, J. A.; Denny, W. A.; Spicer, J. A. Inhibition of the cellular function of perforin by 1-amino-2,4-dicyanopyrido[1,2-a]-benzimidazoles. *Bioorg. Med. Chem.* **2011**, *19*, 4091−4100.

(25) Trapani, J. A.; Ciccone, A.; Browne, K. A.; Smyth, M. J.; Denny, W. A.; Spicer, J. A.; Lyons, D.; Huttunen, K. Benzylidene-2-thioximidazolidinones and Related Compounds, Preparation and Uses Thereof. WO 2011075784, 2011.

(26) Spicer, J. A.; Huttunen, K. M.; Miller, C. K.; Denny, W. A.; Ciccone, A.; Browne, K. A.; Trapani, J. A. Inhibition of the pore-forming protein perforin by a series of aryl-substituted isobenzofuran-1(3H)-ones. *Bioorg. Med. Chem.* **2012**, *20*, 1319−1336.

(27) Mendgen, T.; Steuer, C.; Klein, C. D. Privileged scaffolds or promiscuous binders: a comparative study on rhodanines and related heterocycles in medicinal chemistry. *J. Med. Chem.* **2012**, *55*, 743−753.

(28) Tomasic, T.; Masic, L. P. Rhodanine as a privileged scaffold in drug discovery. *Curr. Med. Chem.* **2009**, *16*, 1596−629.

(29) Pinson, J.; Schmitt-Kittler, O.; Zhu, J.; Jennings, I. G.; Kinzler, K. W.; Vogelstein, B.; Chalmers, D. K.; Thompson, P. E. Thiazolidinedione-based PI3Kα inhibitors: an analysis of biochemical and virtual screening methods. *ChemMedChem* **2011**, *6*, 514−522.

(30) Baell, J. B.; Holloway, G. A. New substructure filters for removal of pan assay interference compounds (PAINS) from screening libraries and for their exclusion in bioassays. *J. Med. Chem.* **2010**, *53*, 2719−2740.

(31) Baell, J. B. Broad coverage of commercially available lead-like screening space with fewer than 350,000 compounds. *J. Chem. Inf. Model.* **2013**, *53*, 39−55.

(32) Tomasic, T.; Masic, L. P. Rhodanine as a scaffold in drug discovery: a critical review of its biological activities and mechanisms of target modulation. *Expert Opin. Drug Discovery* **2012**, *7*, 549−560.

(33) Heng, S.; Tieu, W.; Hautmann, S.; Kuan, K.; Sejer Pedersen, D.; Pietsch, M.; Gütschow, M.; Abell, A. D. New cholesterol esterase inhibitors based on rhodanine and thiazolidinedione scaffolds. *Bioorg. Med. Chem.* **2011**, *19*, 7453−7463.

(34) Debdab, M.; Carreaux, F.; Renault, S.; Soundararajan, M.; Fedorov, O.; Filippakopoulos, P.; Lozach, O.; Babault, L.; Tahtouh, T.; Baratte, B.; Ogawa, Y.; Hagiwara, M.; Eisenreich, A.; Rauch, U.; Knapp, S.; Meijer, L.; Bazureau, J.-P. Leucettines, a class of potent inhibitors of cdc2-like kinases and dual specificity, tyrosine phosphorylation regulated kinases derived from the marine sponge leucettamine B: modulation of alternative pre-RNA splicing. *J. Med. Chem.* **2011**, *54*, 4172−4186.

(35) The authors extend their sincere gratitude to Professor Jonathan B. Baell, both for useful discussion and for subjecting our current series to the PAINS substructure filters.

(36) Trapani, J. A.; Smyth, M. J. Retroviral Vectors Encoding Recombinant Mouse Perforin, Its Expression and Therapeutic Uses Thereof. WO 2005083098 A1, March 1, 2005.

(37) Kobayashi, K.; Sugie, A.; Takahashi, M.; Masui, K.; Mori, A. Palladium-catalyzed coupling reactions of bromothiophenes at the C−H bond adjacent to the sulfur atom with a new activator system, AgNO$_3$/KF. *Org. Lett.* **2005**, *7*, 5083−5085.

(38) Ortwine, D. F.; Malone, T. C.; Bigge, C. F.; Drummond, J. T.; Humblet, C.; Johnson, G.; Pinter, G. W. Generation of N-methyl-D-aspartate agonist and competitive antagonist pharmacophore models. Design and synthesis of phosphonoalkyl-substituted tetrahydroisoquinolines as novel antagonists. *J. Med. Chem.* **1992**, *35*, 1345−70.

(39) Wang, X.-J.; Tan, J.; Grozinger, K. A significantly improved condition for cyclization of phenethylcarbamates to N-alkylated 3,4-dihydroisoquinolones. *Tetrahedron Lett.* **1998**, *39*, 6609−6612.

(40) Fraser, H. L.; Gribble, G. W. A synthesis of 6,11-disubstituted benzo[b]carbazoles. *Can. J. Chem.* **2001**, *79*, 1515−21.

(41) Ran, J.-Q.; Huang, N.; Xu, H.; Yang, L.-M.; Min Lv, M.; Zheng, Y.-T. Anti HIV-1 agents 5: synthesis and anti-HIV-1 activity of some N-arylsulfonyl-3-acetylindoles in vitro. *Bioorg. Med. Chem. Lett.* **2010**, *20*, 3534−3536.

(42) Lopez, J. A.; Susanto, O.; Jenkins, M. R.; Lukoyanova, N.; Sutton, V. R.; Law, R. H. P.; Johnston, A.; Bird, C. A.; Bird, P. I.; Whisstock, J. C.; Trapani, J. A.; Saibil, H. R.; Voskoboinik, I. Perforin forms transient pores on the target cell plasma membrane to facilitate rapid access of granzymes during killer cell attack. *Blood* **2013**, *121*, 2659−2668.

(43) Lopez, J. A.; Jenkins, M. R.; Rudd-Schmidt, J.; Brennan, A. J.; Danne, J. C.; Mannering, S. I.; Trapani, J. A.; Voskoboinik, I. Rapid and unidirectional perforin pore delivery at the cytotoxic immune synapse. *J. Immunol.* **2013**, *191*, 2328−2334.

(44) Lu, T.-J.; Yang, J.-F.; Sheu, L.-J. An efficient method for the acetalisation of α,β-unsaturated aldehydes. *J. Org. Chem.* **1995**, *60*, 2931−2934.

(45) Menet, C. J. M.; Blanc, J.; Hodges, A. J.; Burli, R. W.; Breccia, P.; Blackaby, W. P.; Van Rompaey, L. J. C.; Fletcher, S. R. Preparation of [1,2,4]Triazolo[1,5-a]pyridines as JAK Inhibitors for the Treatment of Degenerative and Inflammatory Diseases. Patent WO 2010010184 A1, January 28, 2010.

(46) Kumar, R.; Chakraborti, A. K. Copper(II) tetrafluoroborate as a novel and highly efficient catalyst for acetal formation. *Tetrahedron Lett.* **2005**, *46*, 8319−8323.